MODELING AND MAXIMUM THEORETICAL EFFICIENCIES OF LINEARLY GRADED ALPHAVOLTAIC AND BETAVOLTALTAIC CELLS

A Thesis presented to the Faculty of the Graduate School
University of Missouri

In Partial Fulfillment
Of the Requirements for the Degree
Master of Science

by
Kyuhak Oh

Dr. Mark A. Prelas
Research Advisor

JULY 2011

The undersigned, appointed by the Dean of the Graduate School, have examined the thesis entitled

MODELING AND MAXIUM THEORETICAL EFFICIENCIES OF LINEARLY GRADED ALPHAVOLTAIC AND BETAVOLTAIC CELLS

Presented by Kyuhak Oh

A candidate for the degree of Master of Science

And hereby certify that in their opinion it is worthy of acceptance.

Dr. Mark A. Prelas

Dr. Tushar K. Ghosh

Dr. Zaichun F. Feng

Dr. Jason B. Rothenberger

To my lovely wife, Jihyen and adorable son, Jeho

ACKNOWLEDGEMENTS

First of all, I would like to thank the Lord Jesus Christ for the continuous love, help and support.

I would like to express my heartfelt thanks to my dear wife, Jihyen, my cute son, Jeho and my respectful parents. Without their love, support, patience, and understanding, which helped to make my study possible, I never would have fulfilled this research.

I would like to express my special appreciation to my advisor, Professor Mark A. Prelas, for valuable advice, continuous guidance and expert help to encourage me during my entire project at this great university, especially for my research related with nuclear battery.

I am indebted to Dr. Jason B. Rothenberger, Eric D. Lukosi, Daniel E. Montenegro, Robert J. Schott, Charles L. Weaver, Denis A. Wisniewski, Matthew L. Watermann, and Elim Ortiz for assisting me in teaching the codes, giving some advices, and discussing my project.

I also would like to thank all the faculty and staff in the Nuclear Science and Engineering Institute for providing me with support and help in various aspects.

Finally, I would like to thank the R.O.K Army for giving me the opportunity to study in the University of Missouri-Columbia. This opportunity will make the Army and I develop in the long run.

TABLE OF CONTENTS

LIST OF FIGURES

LIST OF TABLES

MODELING AND MAXIMUM THEORETICAL EFFICIENCIES OF LINEARLY GRADED ALPHAVOLTAIC AND BETAVOLTAIC CELLS

Kyuhak Oh

Dr. Mark A. Prelas, Research Advisor

ABSTRACT

This thesis presents a study on the optimization of the amount of energy deposited by alpha and beta particles in the depletion region of a silicon carbide (SiC) as alphavoltaic and betavoltaic cells using Monte Carlo models.

Two Monte Carlo codes were used in this study for alpha particles: the Stopping and Range of Ions in Matter/ TRansport of Ions in Matter (SRIM/TRIM) code and the GEometry ANd Tracking simulation of the passage of particles through matter (GEANT4) code. The models examined the transport of 5.307 MeV alpha particles emitted by Polonium-210 (Po-210). Energy deposition in a 1 μm depletion region of SiC was calculated for a spherical geometry using GEANT4, and a slab geometry using both SRIM/TRIM and GEANT4. These geometries were optimized for the maximum possible alphavoltaic energy efficiency. The models, which match very well, indicate that the maximum theoretical energy conversion efficiency, which was optimized for a SiC alphavoltaic cell is approximately 2.1%.

Three Monte Carlo codes were used in the study for beta particles: the GEometry ANd Tracking simulation of the passage of particles through matter (GEANT4) code, the PENetration and Energy LOss of Positrons and Electrons in matter (PENELOPE) code, and the Monte Carlo N-Particle eXtended (MCNPX) code. These codes were used to examine the transportation of beta particles from Yttrium-90 (Y-90), Strontium-90 (Sr-90), and Sulfur-35 (s-35). Both the average beta energy from each source and the entire spectrum were modeled for calculating maximum theoretical energy deposition in both a spherical and slab geometry. A simulated depletion region was added in post processing containing the maximum energy deposited per μm. The calculated maximum efficiencies are approximately 1.99 %, 0.31 %, and 0.02 % using mono-energetic average energy and 1.32 %, 0.21 %, and 0.02 % using an energy spectrum for S-35, Sr-90, and Y-90, respectively.

This study provides a useful guide for the upper limit of expected efficiency for alphavoltaic and betavoltaic cells using a linearly graded semiconductor.

CHAPTER 1. INTRODUCTION

1.1. Reason for Research

Nuclear battery research, which dates as far back as 1913,[1] has experienced a recent renaissance, where alpha and beta voltaic batteries have been the primary focus. These cells typically use a linearly graded *p*-*n* junction. The goal of this research is to study idealized alphavoltaic and betavoltaic systems, where the transport of alpha and beta particles is studied to determine the optimum geometry that produces the maximum useable current (or energy production) for direct irradiations of a linearly graded semiconductor. The fabrication challenges for solid state nuclear batteries are complex in that it involves matching the transport scale length of the alpha and beta particles to the scale length of the energy conversion system.[2] Recent studies demonstrate a mismatch of the fundamental scale lengths of the system, limiting the efficiency of the device. This study was conducted to provide a useful guide for the maximum theoretical efficiency of alphavoltaic and betavoltaic cells based on well-benchmarked Monte Carlo models. This is important, because there are many reports in the literature of efficiencies that appear to be very high.[3-5] The results of this work provide a guideline and a methodology for the reader to evaluate such reports and to determine whether true efficiencies are being reported, or if experimental error may be an issue.

Nuclear battery technology is crucial for long-lived, portable power generating sources in applications where other power sources such as solar cells and chemical batte-

ries are not suitable. Examples of these applications are mobile sensor platforms, power sources for remote instruments, and military electronic systems. An alphavoltaic is a photovoltaic (PV) cell powered by impinging alpha particles in a *p*-*n* junction diode (or transducer). A Betavoltaic is a generator of electrical current, in effect a form of battery, which use energy from a radioactive source emitting beta particles instead of alpha particles. Electron-hole pairs are created from these impinging particles in the depletion region (i.e., the interface of the *p*-type and *n*-type regions) or can diffuse to the region.[6] The Fermi potential separates the electrons and holes resulting in an electrical current. The thickness of the depletion region in a typical SiC PV cell is approximately 1 μm.[7, 8] The model presented here examines the transport scale length and the energy deposition of alpha and beta particles in the semiconducting material structure.

Alpha particles and sources are relatively well behaved in that an alpha source is mono-energetic and the track of an alpha particle is nearly linear. As a consequence, the electron-hole pair production in the medium is predictable because it follows the Bragg curve. In contrast, beta particles and sources are not as well behaved, being emitted with a given energy spectrum and following a non-linear path in matter. As a result, pair production in a medium is not as predictable as with alpha particles. Thus, modeling betavoltaic cells has additional complexities. Additionally, alphavoltaic and betavoltaic cells are subject to intense radiation damage from the particles and have lifetime issues.[6] There are some similarities between alphavoltaics and betavoltaics. The problem of matching the range of the beta particle in the medium to the scale length of the transducer used for energy conversion is the underlying problem for both radiation types. However, due to

the increased range of the higher energy beta particles, the mismatch between the range of the radiation and the scale length of the transducer is even more pronounced for betavoltaics. Additional inefficiency is attributed to the broad energy spectrum of beta particle emission from the source, which makes it very difficult to harvest energy by depositing energy in a relatively narrow physical space (i.e. depletion region) in a betavoltaic. It will be shown that beta particles of different energy have very different regions where maximum pair production rate exists.

In this study, the alphavoltaic and betavoltaic cells will be based on a commonly used material, SiC.[9] To explore this issue, Po-210 alpha source was simulated in an idealized slab and spherical alphavoltaic system using an energy of 5.307 MeV. Y-90, Sr-90, and S-35 beta sources were modeled under same conditions using their maximum energy, average energies calculated by the 1/3 β_{max} rule and spectrum data, and true energy emission spectra.

1.2. Background on Monte Carlo Codes

SRIM/TRIM[10] is a code which calculates a variety of parameters for ions interacting with matter at energies up to 2 GeV based on Monte Carlo method. This code is used for calculating the distribution of the ions and kinetic effects related to the loss of ion energy through the interaction of ions with matter such as target damage, sputtering, ionization and phonon production. SRIM/TRIM assumes that the ions are mono-directional and mono-energetic. SRIM/TRIM allows for adjusting input beam data such as beam size, emittance, energy-spread and dispersion effects. It is also possible to simu-

late the beam-transport including scattering and collimating elements. This code is very convenient to use. The calculated data can be plotted in real time, saved, and displayed as needed. The data in SRIM is reliable since it has been benchmarked with data from the other Monte Carlo codes as well as experiments. Since its introduction in 1985, SRIM/TRIM has been upgraded about every six years. The SRIM/TRIM database has 2,800 additional data sets added to its original database in 2010 through experiments, so it has over 28,000 values of stopping power and range. With these characteristics, SRIM/TRIM has been used in the nuclear and chemical fields to model ion interactions with matter.

GEANT4[11, 12] is a tool kit for the simulation of the interaction of particles through matter across a very wide energy range from 250 eV to 1 PeV or more, using Monte Carlo methods. It has many kinds of functions such as graphical presentations of detector geometries and shower development, usage of a wide variety of particles from geantinos, which are the virtual particle you can design in GEANT4, to heavy ions, easy control of interaction physics, tracking, stepping, geometry, physics models and hits, and description of the most complicated and realistic geometries. Further, this tool kit is available to all at no cost. With these characteristics, it has been used in high energy physics, nuclear and radiation computations, space applications related to the natural space radiation environment and medical physics for treatment. GEANT was first developed in the 1970s. In 1982, it was written in the Fortran language and developed to GEANT3but had difficulties because of the need to add new physics models to the existing models. Finally, GEANT4 was developed by CERN and KEK in 1993, written in the

C++ program and object-oriented. Since the sources of GEANT4 data have been derived from the collaboration of physicists and software engineers from many cooperating institutes and universities across the world, there have been many accumulated results and experiences related to the field of physical processes using Monte Carlo simulations. Thus, GEANT4 is a well developed and well benchmarked tool for modeling of charged particle interactions.

PENELOPE,[13] based on a scattering model with combination of numerical databases of analytical cross-section models, is a widely available general purpose Monte Carlo simulation code of coupled electron-photon transport, which is implemented in FORTRAN 77 and distributed by the OECD NEA Data Bank. It can be applicable with energies ranging from a few hundred eV up to 1 GeV and for arbitrary materials and complex geometries that has been developed at the Universitat de Barcelona over the last 20 years. Besides, PENELOPE permits a good description of the particle transport at the interfaces and presents a more accurate description of the electron transport at low energies in comparison to other general purpose MC codes. In PENELOPE, electrons and positrons are simulated by means of a mixed scheme where collisions are classified as "hard" (i.e., interactions with energy loss and angular deflection greater than preselected cutoff values) and "soft" (i.e., interactions with energy loss and angular deflection below the preselected cut-off values). Thus, this code is usually used to calculate for elastic scattering and inelastic collisions of electrons and positrons, bremsstrahlung emission by electrons and positrons, inner-shell ionization by electron and positron impact, positron annihilation, coherent (Rayleigh) scattering, , incoherent (Compton) scattering and pho-

toelectric absorption of photons, and electron-positron pair production. A geometry package called pengeom permits the generation of random electron-photon showers in material systems consisting of homogeneous bodies limited by quadric surfaces (i.e. planes, spheres, cylinders, etc.)

MCNPX[14] is a Fortran90 Monte Carlo radiation transport code with continuous-energy transport of many particles and light ions in arbitrary materials. Like PENELOPE, the MCNPX code allows arbitrary 3D configurations of user-defined materials in geometric cells bounded by intersections. The upper energy limits for electrons and photons are 1 and 100 GeV, respectively and a lower limit of 1 keV is fixed for these particles. It contains flexible source and tally options, interactive graphics, and support for both sequential and multi-processing computer platforms. The official release date of MCNPX 2.6.0 is April 30, 2008. MCNPX began in 1994 as a code-merger project of MCNP 4B and LAHET 2.8 and released to the public in 1999. In 2002, it was upgraded to MCNP4C and has been developed to most MCNP5 capabilities. MCNP is a highly stable code for tracking neutrons, photons and electrons, and using evaluated nuclear data libraries for low-energy interaction probabilities. MCNPX has extended this base to a comprehensive set of particles and light ions, with heavy ion transport in development.

CHAPTER 2. ALPHAVOLTAIC

2.1. Model Specification

There are only a few codes suitable for modeling alpha particle interactions. The two codes chosen in this study which treat the interaction of the alpha particle with matter for the nuclear battery area are SRIM/TRIM[10] and GEANT4.[11, 12] SRIM/TRIM assumes that the mono-directional and mono-energetic ions interact with matter in only the slab geometry. Work transporting protons and comparing results from GEANT4 and MCNPX demonstrates GEANT4's versatility with ions.[14, 15]

The first model used in this study was based on the optimal geometrical configuration for a mono-energetic isotropic alpha source. The alpha source was placed at the center of a spherical PV cell (Fig. 1). The optimum energy production will occur when the electron-hole pair formation is maximized in the depletion region. Therefore, the maximum energy output will occur when the specific ionization is a maximum within the 1 μm depletion region of linearly graded *p*-*n* junction transducer. GEANT4 was used for creating the experimental model as well as for finding the maximum production of electron-hole pairs in the depletion region.

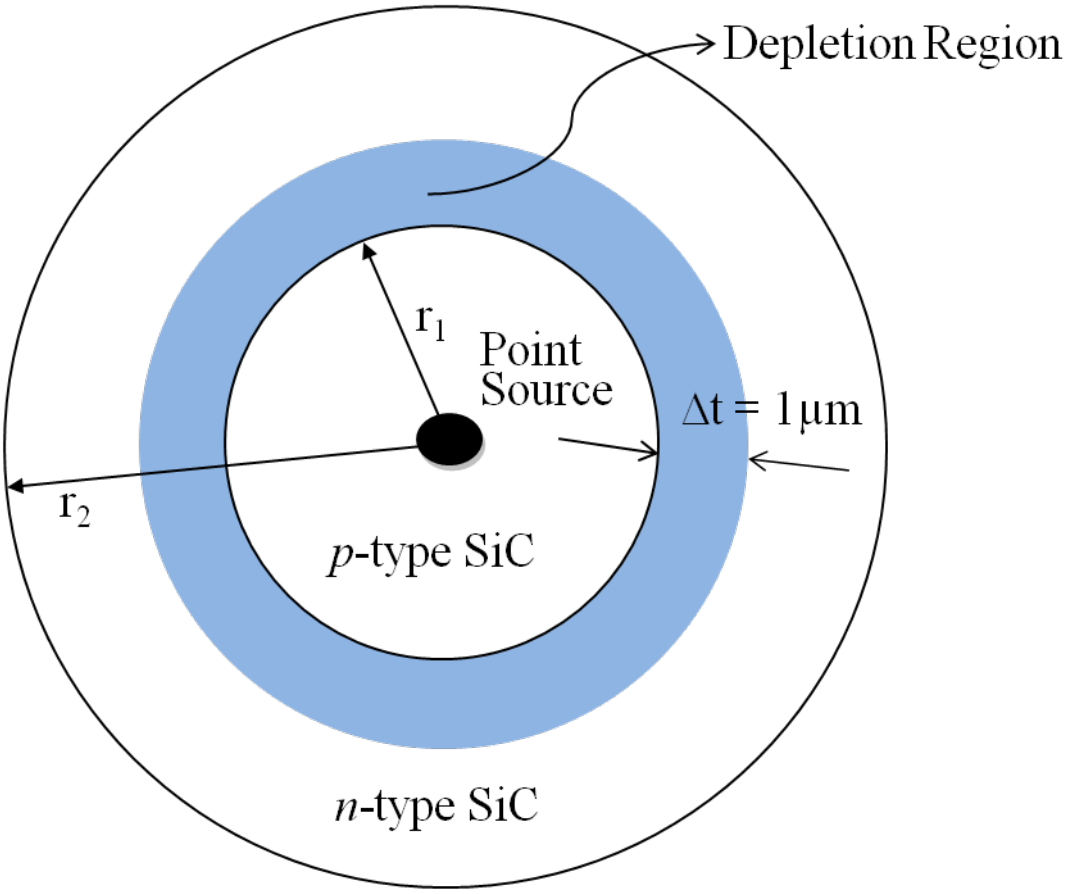

Figure 1: Optimized geometrical SiC alphavoltaic cell using a spherical geometry and a depletion region with a point alpha source at the center

A second model using a mono-energetic alpha beam impinging on a slab diode was developed as a means of benchmarking GEANT4 to a well established code, SRIM/TRIM (Fig. 2). The model was used to predict the maximum electron-hole pair production rate in the depletion region.

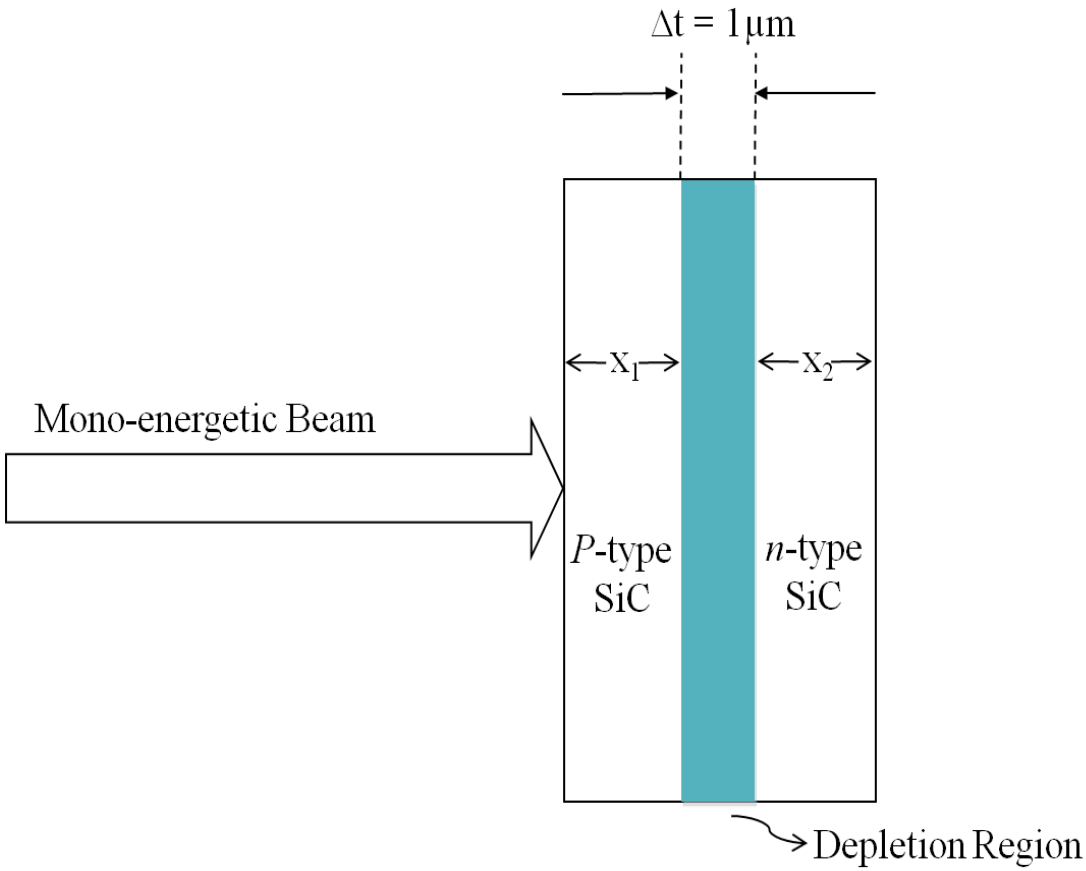

Figure 2: Slab model used for benchmarking GEANT4 with SRIM/TRIM. A mono-directional, mono-energetic alpha beam impinges on the slab target

SiC was chosen because it is a wide band-gap ($E_g \approx 3.0$ eV) material which has some radiation resistance,[9] and it also has a very low current leakage. Thus, it has been considered a viable base material for nuclear battery research.[5, 16, 17] There are two pre-dominant crystal structures, 4H-SiC and 6H-SiC. In this model, the 6H-SiC structure was used.

The alpha source chosen for this study was the alpha emitter, Polonium-210 (Po-210). It has a half-life of 138.38 days and is subject to less regulatory constraints than Am-241 or Pu-238. It is also more widely available than Gd-148.[18] Po-210 decays to Pb-

206 through the emission of an alpha particle with an energy of 5.307 MeV by the following reaction,

$$^{210}_{84}Po \rightarrow {}^{206}_{82}Pb + \alpha + 5.307\ MeV \quad (1)$$

As alpha particles interact with the medium, low energy (~ 1 keV) secondary electrons are created.[19] The secondary electrons then interact with the medium to create tertiary and higher order electrons, and the electron yield is proportional to the specific ionization of the material.[20, 21] The energy flow of secondary products from alpha particle interactions follows the principle of detailed energy balance. If the energy lost due to secondary ionizations from one cell into an adjacent cell equals the energy lost from the adjacent cell to the original cell, then the energy deposition in the cell will be equal to the energy deposited by the alpha particles. Since the depletion region is at the Bragg peak, the assumption of the principle of detailed energy balance overestimates the electron-hole production, thus providing a theoretical maximum limit for electron-hole pair production.

The slab geometry used a mono-directional beam, which was incident perpendicularly to the slab-shaped PV cell (Fig. 2). The spherical model, in contrast, used an isotropic point source at the center of a spherical PV cell. Both configurations are optimal in order to harvest the maximum amount of the alpha particle energy from the source. Even though it may not be possible to produce the hypothetical spherical PV cell, it does represent the most efficient configuration for transporting alpha particles from an isotropic alpha source to the depletion region because of the linear path of the alpha particles slowing down in the material. Thus, the results from this optimized geometry provide an upper limit for the overall efficiency of the alphavoltaic cell.

Using SRIM/TRIM, it was demonstrated that all of the alpha energy is deposited within approximately 20 µm. Thus, twenty 1 µm thick cells were used in GEANT4 calculations for both the slab and sphere geometries. The location of the depletion region to optimize the energy harvested in the cell can be determined through such simulations.[7]

2.2. Results

The SRIM/TRIM results from the SiC slab model show that the peak of the Bragg curve occurs at around 16 µm. Figure 3 illustrates the tracks of alpha particles within the slab and demonstrates their relatively linear paths. Figure 4 shows the alpha particle's Bragg curves in the SiC target.

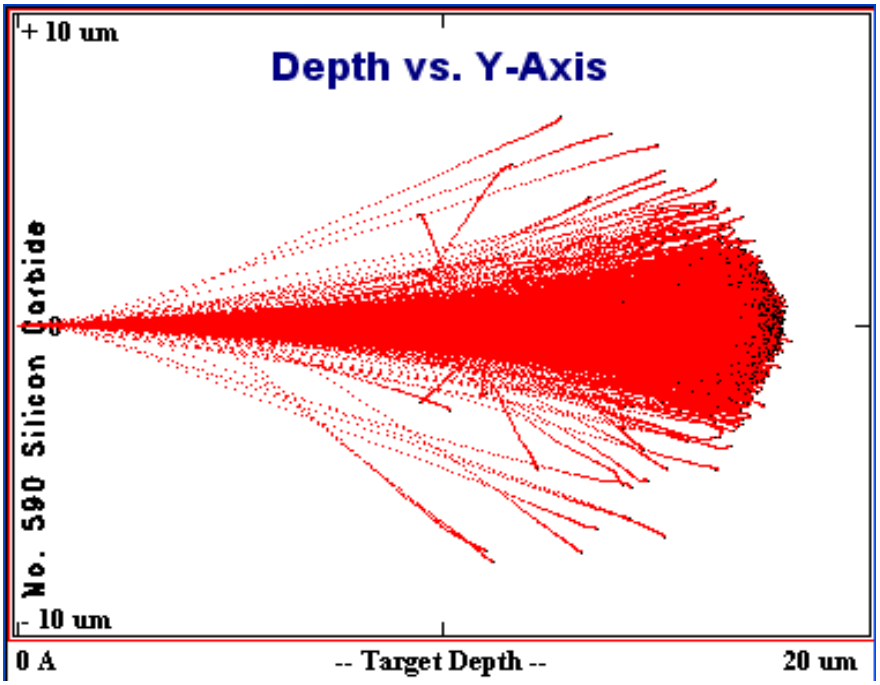

Figure 3: Illustration the tracks of Po-210 alpha particles within the SiC slab using SRIM/TRIM

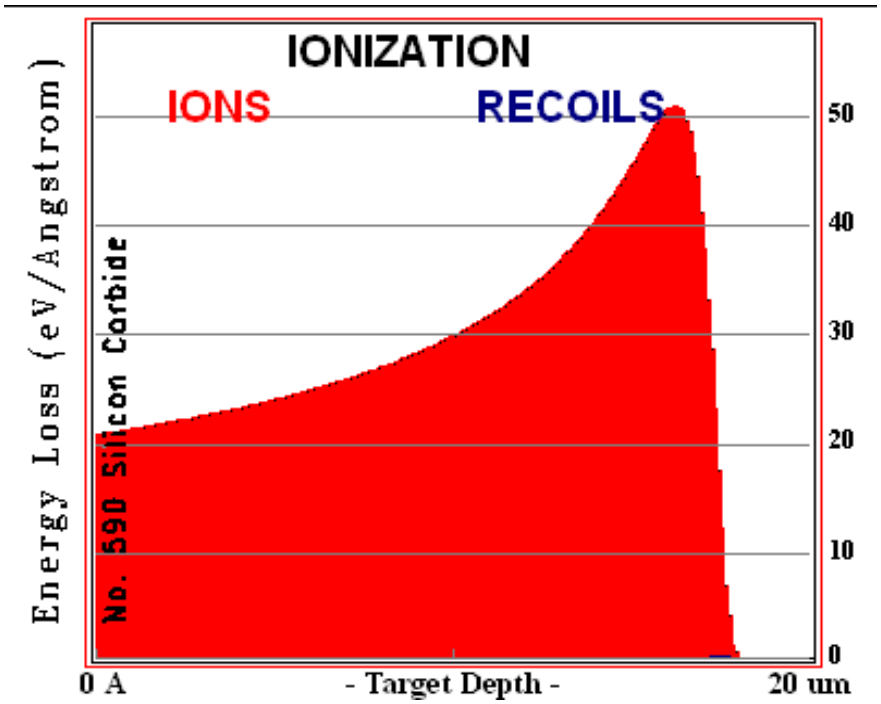

Figure 4: The alpha particle's Bragg curves at in the SiC target using SRIM/TRIM

Figure 5 shows the alpha tracks in the SiC slab using GEANT4 and compares well with Fig. 3. Figure 6 depicts the alpha tracks in a SiC sphere using GEANT4 with the isotropic point source at the center. Because of the spherical symmetry in this configuration, the alpha particle paths traverse away from the point source into the surrounding material.

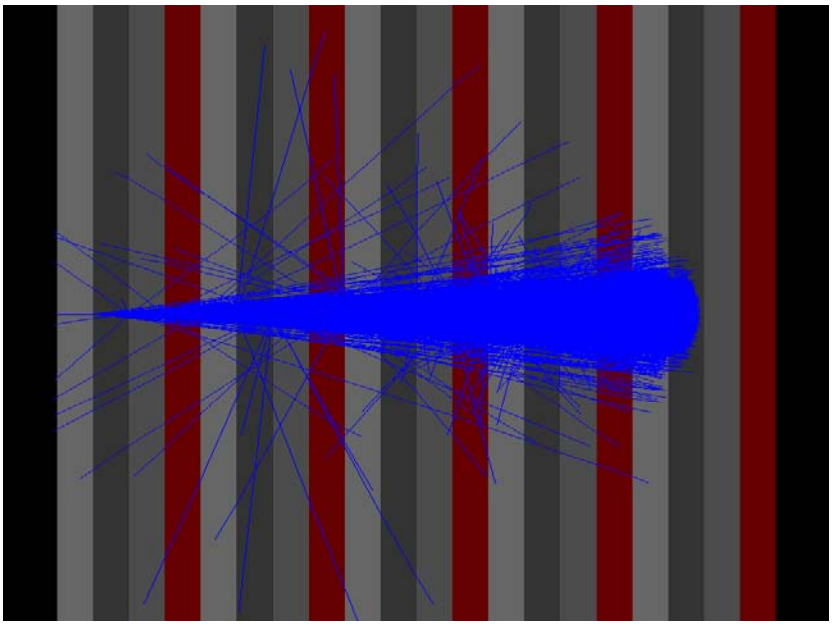

Figure 5: Simulation of Po-210 Alpha Decay into SiC of Slab Model

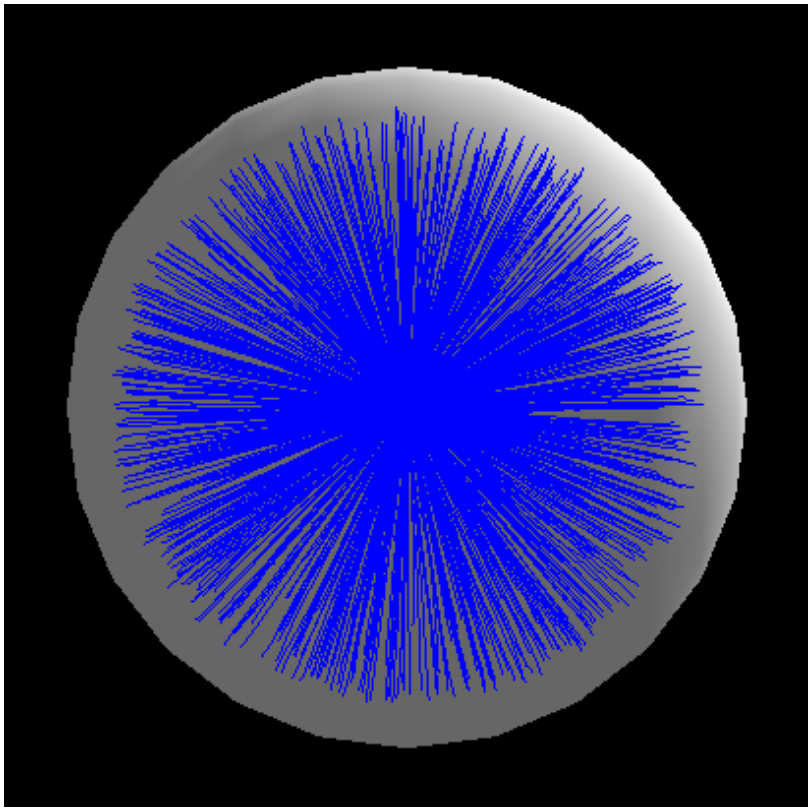

Figure 6: Simulation of Po-210 Alpha Decay into SiC of the Sphere Model

The energy deposition in SiC is a function of distance in both the slab and sphere geometries is shown in Fig. 7. The peak of the energy deposition is observed at the depth of about 16 µm. The SRIM/TRIM and GEANT4 results are consistent for the slab model.

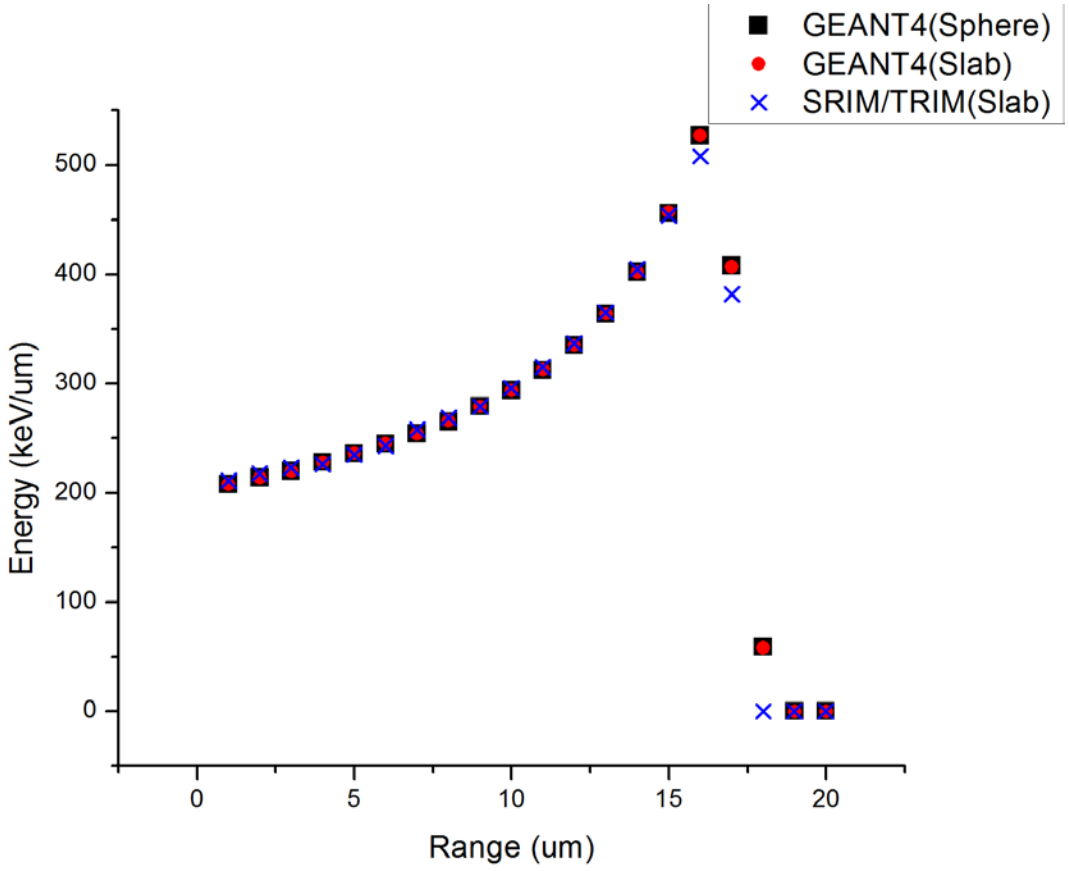

Figure 7: Alpha particle energy deposition vs. distance in the slab model using SRIM/TRIM and in the slab and sphere models using GEANT4

Table 1 shows the deposited energies in each of the defined cells in the model. The energy deposition rate follows the typical Bragg curve which peaks near 16 µm. Beyond the Bragg peak, the energy deposition drops sharply. In addition, the table shows

that the maximum energy deposition in a 1 μm layer occurs between 15 to 16 μm from the source. The percentage of energy deposited is consistent for both the slab and the spherical models. GEANT4 predicts that the energy deposited in this layer is ~ 9.93 % for the spherical configuration and ~ 9.94 % for the slab configuration. SRIM/TRIM's value for the slab model is ~ 9.57% which is consistent with the GENT4 calculation.

Table 1: GEANT4 and SRIM/TRIM Calculations for Predicting Energy Deposition in a Depletion Region of 1 μm Thick for the Slab and Sphere Models

Range (μm)	GEANT4						SRIM/TRIM	
	Sphere			Slab			Slab	
	Energy (keV)	% deposited	σ (%)	Energy (keV)	% deposited	σ (%)	Energy (keV)	% deposited
0-1	208	3.92	0.006	208	3.92	0.006	211	3.98
1-2	214	4.03	0.006	214	4.03	0.007	218	4.11
2-3	220	4.15	0.006	220	4.15	0.007	223	4.19
3-4	228	4.29	0.006	228	4.29	0.007	226	4.26
4-5	236	4.44	0.006	236	4.45	0.007	235	4.42
5-6	245	4.61	0.006	245	4.61	0.007	243	4.59
6-7	254	4.79	0.006	254	4.79	0.007	258	4.85
7-8	265	5.00	0.006	266	5.00	0.007	269	5.06
8-9	279	5.25	0.006	279	5.25	0.007	279	5.25
9-10	294	5.55	0.006	294	5.55	0.007	296	5.58
10-11	312	5.89	0.006	313	5.89	0.007	315	5.94
11-12	335	6.32	0.006	335	6.32	0.006	337	6.35
12-13	364	6.86	0.005	364	6.86	0.006	365	6.88
13-14	402	7.58	0.006	402	7.58	0.006	405	7.62
14-15	456	8.60	0.006	457	8.61	0.006	454	8.56
15-16	527	9.93	0.006	527	9.94	0.006	508	9.57
16-17	408	7.68	0.017	407	7.66	0.017	382	7.19
17-18	59	1.12	0.118	58	1.09	0.121	0	0.00
18-19	0	0.00	-	0	0.00	-	0	0.00
19-20	0	0.00	-	0	0.00	-	0	0.00
TOTAL	5307	100.00	-	5307	100.00	-	5220	98.40

Assuming that the thickness of the depletion region in the semiconductor structure is about 1 μm, the maximum energy transport efficiency (η_d) from Table I is 9.93% for the spherical configuration, and 9.94% for the slab configuration based on GEANT4, and 9.57% from the slab configuration based on SRIM/TRIM.

2.3. Determination of the Maximum Theoretical Efficiency

The energy deposition from radiation is a very important parameter for nuclear batteries.[22] However, there are more factors beyond the total energy deposition to be considered when determining the efficiency of the nuclear battery.

The overall efficiency of the alphavoltaic cell (η_α) is composed of multiple factors. The first of these factors is the maximum energy transport efficiency (η_d), which already appeared above. The second factor is the pair production efficiency (η_{pp}), which is the fraction of deposited energy used in the production of an electron-hole pair. This is the ratio of the ionization potential (*I*), or alternately, the band-gap (E_g) of the material to the *W* value.

$$\eta_{pp} = (E_g/W) \tag{2}$$

The remaining factor accounts for the driving potential efficiency (η_{dp}). This is ratio of the energy gained by an electron driven by the open circuit voltage (V_{oc}), in electron volts, to the energy required to move an electron from the valence band to the conduction band (E_g), in electron volts.[6]

$$\eta_{dp} = (V_{oc}/E_g) \tag{3}$$

Therefore, the total efficiency of an alphavoltaic is,

$$\eta_\alpha = \eta_d \eta_{pp} \eta_{dp} \quad (4)$$

The theoretical maximum energy efficiency can now be determined by the energy transport efficiency values calculated from the optimized slab and spherical models. For conventional alphavoltaic cell structures, the isotropic source will be randomly distributed on the surface, or in a volume in close proximity to the *p*-*n* junction. Thus the alpha emitters are distributed in a way such that the bulk of the particles are not directed in the optimal direction or located at the optimal distance to the depletion region of the cell. So by choosing the optimized spherical configuration, the theoretical maximum efficiency for an alphavoltaic cell can be found. Thus, no cell using a linearly graded PV should exceed this limit.

The alpha source in the slab and spherical models used in this study was directed in the optimal direction and located at the optimal distance from the depletion region (i.e., the alpha sources used were either infinitely thin or point sources for the slab and spherical geometries, respectively). Thus, the maximum possible energy transport efficiency, η_d, obtained from Table 1 is 9.81 % (average value of three results). The pair production efficiency, η_{pp}, for SiC is 0.42.[23] The driving potential efficiency for an optimized PV cell, η_{dp}, will generally not exceed 0.5. Assuming that the electrons are transported through the material without energy loss, the theoretical maximum efficiency of an alphavoltaic cell in an optimum geometry for an isotropic point source is,

$$\eta_\alpha = 9.81 \times 0.42 \times 0.5 \approx 2.1\ \% \quad (5)$$

As discussed, typical alphavoltaic cell designs do not optimize the direction of the alpha particles or the distance that the alpha particles travel before stopping. Thus, a typi-

cal alphavoltaic cell based on a linearly graded *p*-*n* junction will have much lower efficiency than the theoretical maximum.

CHAPTER 3. BETAVOLTAIC

3.1. Model Specification

Three codes chosen for this study which treat the interaction of the beta particle with matter are GEANT4,[11, 12] PENELOPE,[13] and MCNPX.[14] Two models were conducted in this study. The first model was based on an idealized spherical geometrical configuration, where an isotropic beta source was placed at the center of the betavoltaic sphere thus fixing the distance from the source to the depletion region.[24] Although this configuration is not a possible configuration for real betavoltaic systems, it will provide an upper limit to the maximum energy conversion for any configuration. The optimum energy production will occur when electron-hole pair production is maximized in the depletion region. Thus, the model is adjusted such that the radius, denoting the depletion region, is centered at the location of maximum electron-hole pair generation.[24] A second model utilized a slab geometry with a mono-directional beta beam incident parallel to the normal of the SiC slab.[24] This model was also used to predict the location of the maximum electron-hole pair production rate in the depletion region.

The beta sources simulated in this study were Y-90, Sr-90, and S-35. The use of the three sources permits an approximation of the total energy of the battery which is dependent on the half-life, specific activity, and particle energy spectrum of the source. Both Y-90 and Sr-90 are good for long life applications. S-35 has a lower decay energy, a

shorter half-life, higher activity (or power density), and it can be readily incorporated into a semiconductor device.[25, 26] Characteristics of each isotope are compared in Table 2.

Table 2: Radioisotope sources for a betavoltaic cell

Isotope	Half-Life	Max Energy	Average Energy		Daughter Isotope
			1/3 β_{max} rule	spectrum	
S-35	87.51 days	167.47 keV	55.8 keV	53.1 keV	Cl-35
Sr-90	28.8 years	546 keV	182 keV	167 keV	Y-90
Y-90	2.67 days	2.28 MeV	760 keV	945 keV	Zr-90

Average beta energy has been used in prior betavoltaic models.[27] In this study, results from max beta energy, average beta energies by 1/3 β_{max} rule and spectrum data, and the full beta spectrum were examined and compared. The maximum energy deposition in the depletion region was found providing an upper limit to the energy transport efficiency.

As with the prior study on alphavoltaics,[24] SiC was selected because it is a commonly used as a base material in nuclear battery research.[5, 16, 17] Using these three codes with max beta energy, it was shown that the ranges of the beta particles from S-35, Sr-90, and Y-90 are about 120, 700, and 4000 μm and almost all of the beta particle energies are dissipated over the specified ranges cited. When using the average energy by 1/3 β_{max} rule, it was shown that the ranges of beta particles of S-35, Sr-90, and Y-90 are about 24, 140, and 1200 μm. Using the average energy by beta energy spectrum, it was shown that the ranges of the beta particles from S-35, Sr-90, and Y-90 are about 20, 120, and 1600 μm. Higher energy beta particles have a larger range. If the beta energy spectra are consi-

dered, at the maximum beta energy the ranges for S-35, Sr-90, and Y-90 are approximately 80, 400, and 3000 µm. The number of layers for the modeling was chosen based on the beta particle range. For the model using the max beta energy, 120, 700, and 4000 layers each with a thickness of 1 µm was used. For the model using the average beta energy by 1/3 β_{max} rule, 24, 140, and 1200 layers each with a thickness of 1 µm was used. For the model using the average beta energy by energy spectrum, 20, 120, and 1600 layers each with a thickness of 1 µm was used. For the full spectrum model, 80, 400, and 3000 layers each of thickness of 1 µm was used.

3.2. Results

In contrast to alpha particles, which traverse in a nearly linear path through SiC material, beta particles deflect by scattering events and follow a highly non-linear path in the medium due to their lower mass. Figure 8 illustrates the tracks of beta particles within the slab and demonstrates their relatively random-walk like paths. Figure 9 depicts the beta tracks in a SiC sphere with the isotropic point source at the center. Because of the spherical symmetry in this configuration, the beta particle paths traverse away from the point source into the surrounding material. In Fig. 8 & 9, the electromagnetic radiation created by bremsstrahlung, as well as beta particles, are observed.

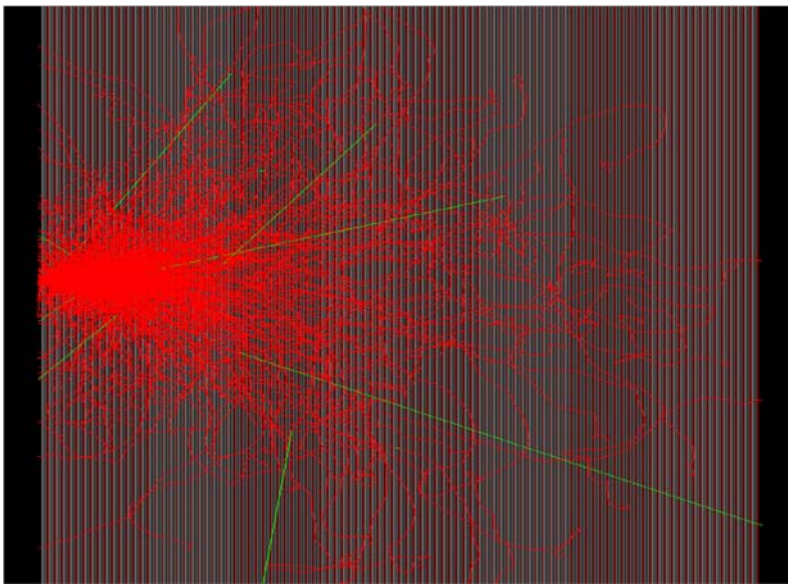

Figure 8: GEANT4 simulation of Sr-90 Beta Decay into SiC of Slab

The beta tracks are illustrated by the red lines and the bremsstrahlung photons are illustrated by the green lines.

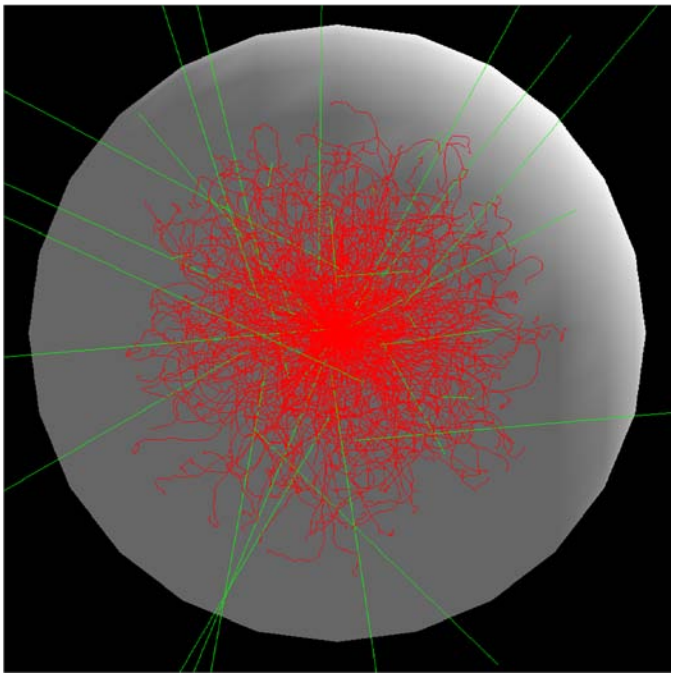

Figure 9: GEANT4 simulation of Sr-90 Beta Decay into SiC of Spherical Model

The beta tracks are illustrated by the red lines and the bremsstrahlung photons are illustrated by the green lines.

3.2.1 Max beta energy

The models examined the transportation of maximum energy beta particles at 2.28 emitted by a Y-90 source, at 0.546 MeV emitted by a Sr-90 source and at 0.167 MeV emitted by a S-35 source in SiC slab and sphere geometries. The energy deposition in SiC as a function of distance in the slab and sphere model is shown in Fig. 10-15. The peaks of the energy deposition in all three codes agree well for both the slab and the sphere models regardless of source types.

When comparing both graphs in the slab and the sphere models, the peaks are shown at different places. The explanation for the differences is that when an electron back-scatters in a slab geometry, it can be lost when it exits the surface while a back-scattered electron is not lost in a spherical geometry. Therefore, electrons in the slab geometry that back-scatter are potentially lost and not allowed to deposit additional energy, whereas a back-scattered beta remains in the spherical geometry and deposits all of its energy. However, the peak location in the sphere geometry lies deeper into the SiC than in the slab geometry. This can be explained by the coordinate system used in the two models. As an example, consider two electrons that travel the exact same path with respect to its entering location. In the slab geometry case, when an electron leaves the surface, the location that the electron escapes is at the starting point, or at r equal to zero. In the spherical case, however, the electron that would have escaped in the slab geometry is located at a value of r greater than zero. In this case, then, the energy deposited by this electron during its escape route is bigger in a location deeper into the sphere than the slab

geometry. In addition, the electron persists in the spherical geometry and deposits additional energy.

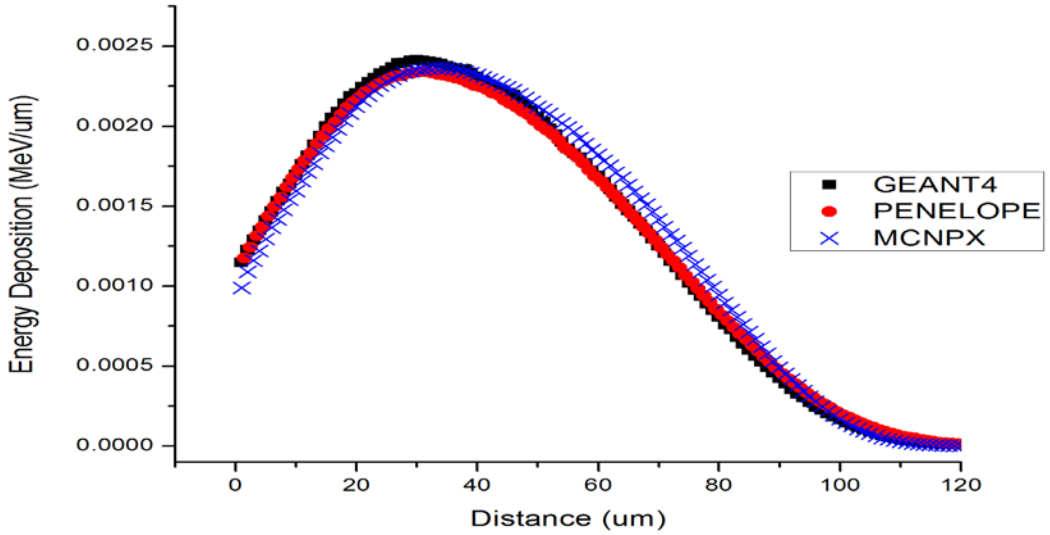

Figure 10: Simulated energy deposition by max beta energy versus distance in the slab geometry using GEANT4, PENELOPE, and MCNPX codes for S-35

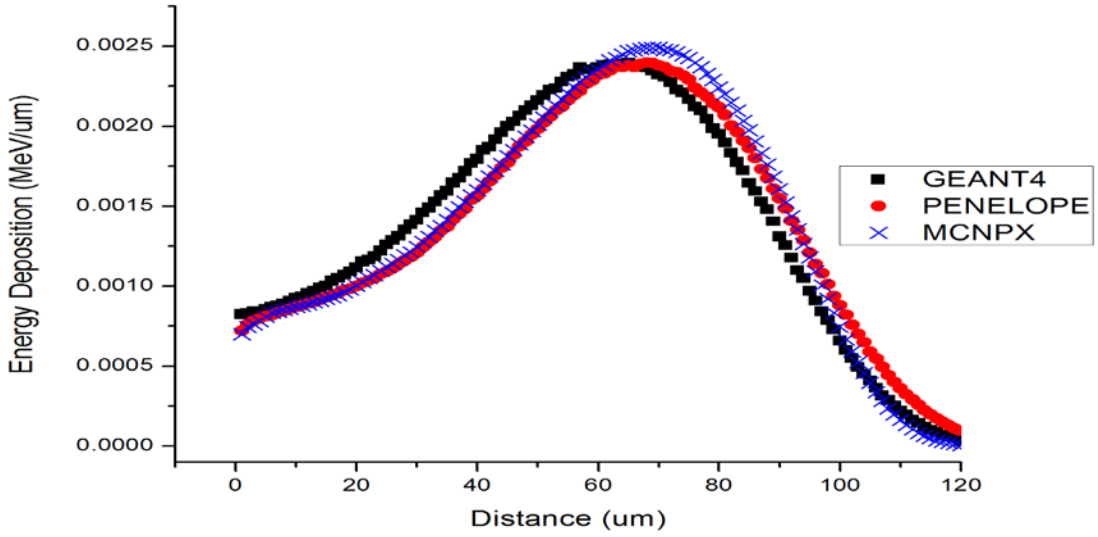

Figure 11: Simulated energy deposition by max beta energy versus distance in the sphere geometry using GEANT4, PENELOPE, and MCNPX codes for S-35

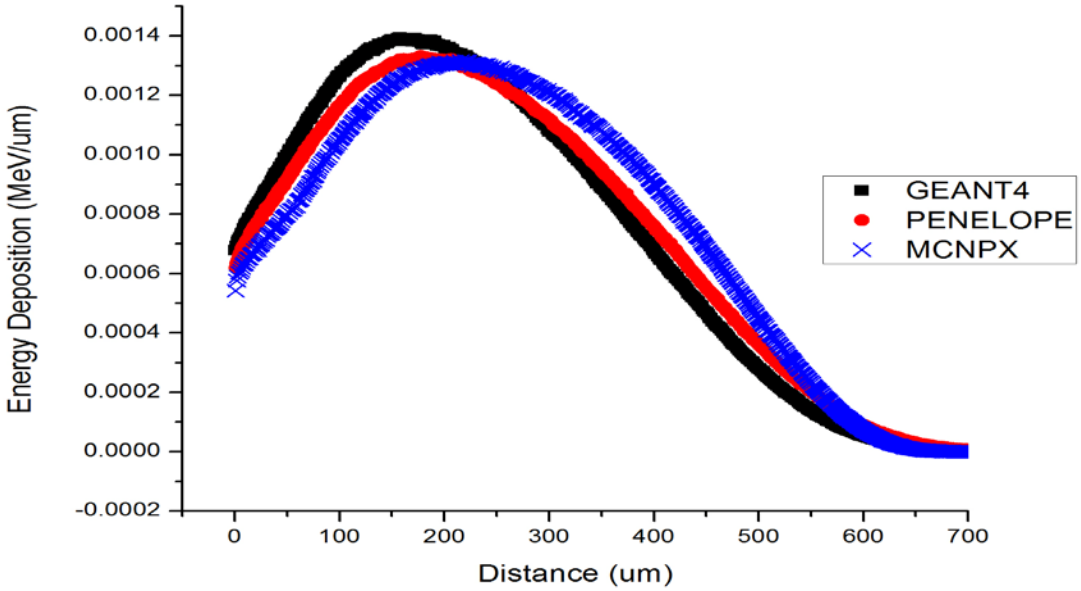

Figure 12: Simulated energy deposition by max beta energy versus distance in the slab geometry using GEANT4, PENELOPE, and MCNPX codes for Sr-90

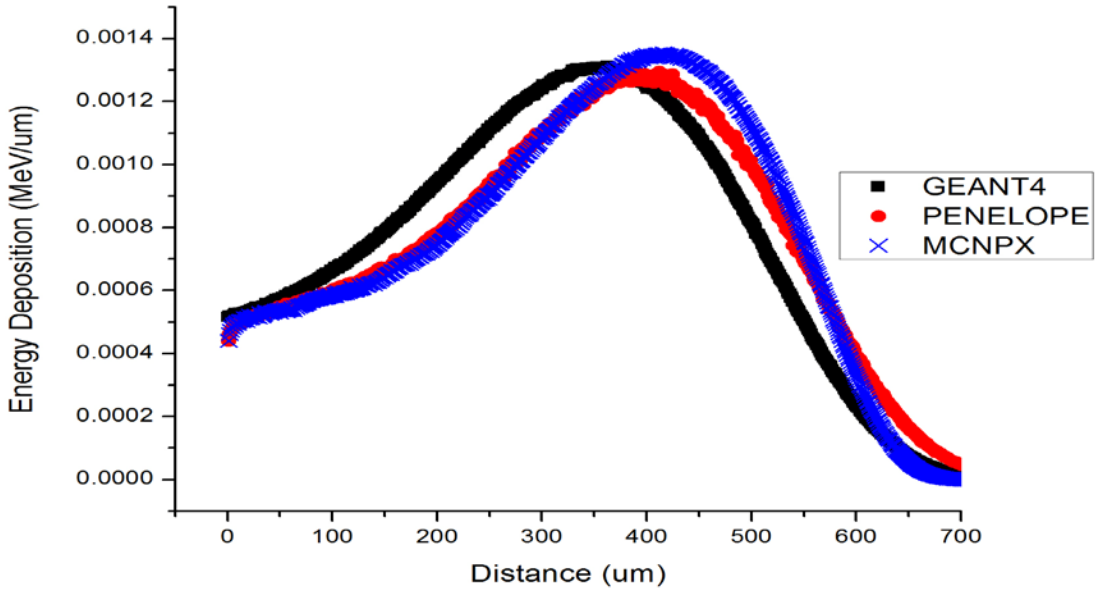

Figure 13: Simulated energy deposition by max beta energy versus distance in the sphere geometry using GEANT4, PENELOPE, and MCNPX codes for Sr-90

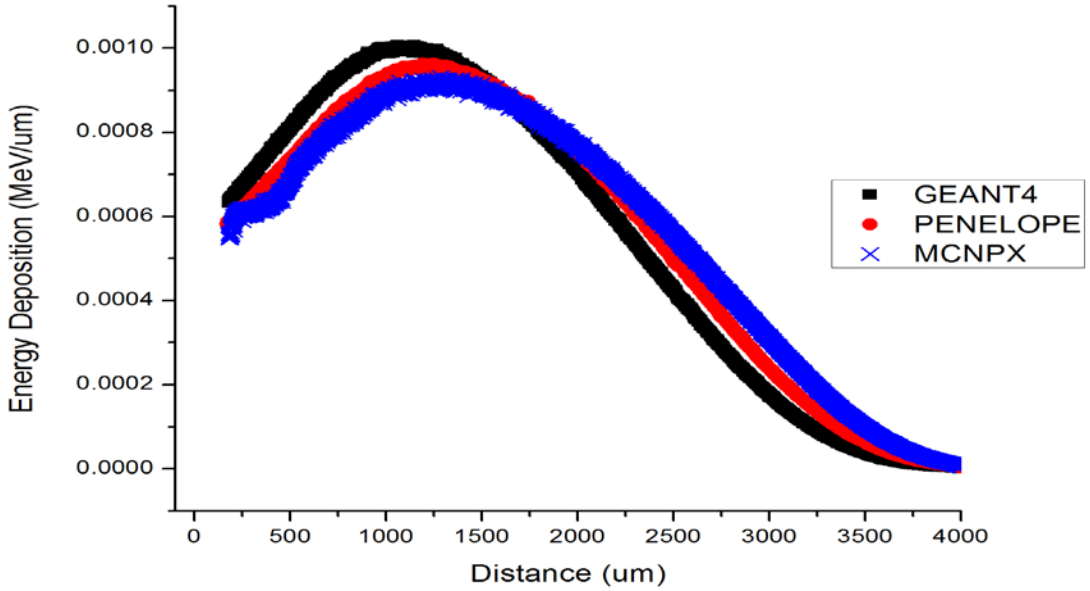

Figure 14: Simulated energy deposition by max beta energy versus distance in the slab geometry using GEANT4, PENELOPE, and MCNPX codes for Y-90

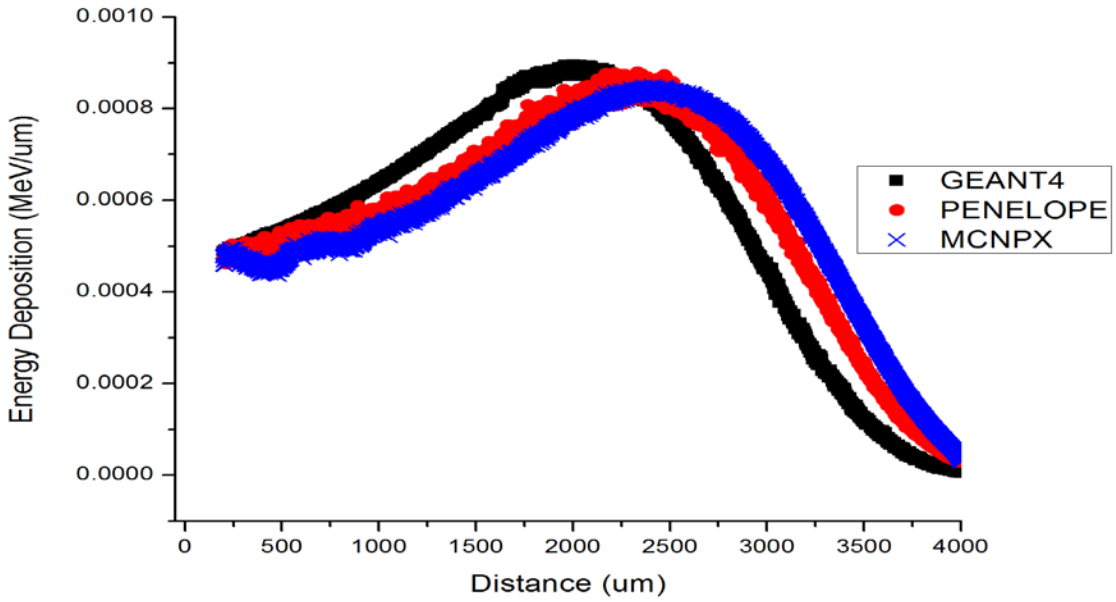

Figure 15: Simulated energy deposition by max beta energy versus distance in the sphere geometry using GEANT4, PENELOPE, and MCNPX codes for Y-90

Table 3 shows the deposited energies in the depletion zone from each model and each source. In addition, the table show that the maximum percentage of energy that is deposited in 1 μm depletion region of the SiC. The percentages of energy deposited are consistent for both the slab and the spherical models. Three codes predict that the average deposited energy efficiencies in the 1 μm thick depletion region are 1.42 % for the slab configuration and 1.46 % for the sphere configuration when using S-35 source. These values for the slab model and the sphere model using Sr-90 are 0.24 % and 0.24 %. Finally, the efficiencies using Y-90 source are 0.04 % with slab geometry and 0.04 % with sphere geometry.

Table 3: Range at which the peak energy deposition occurs, peak energy deposition, and efficiency calculations of S-35, Sr-90, and Y-90 sources with max energy in both slab and sphere geometries using GEANT4, PENELOPE, and MCNPX codes

Source	Geometry	Contents	GEANT4	PENELOPE	MCNPX	Average
S-35	Slab	Range at Max Energy (μm)	30	31.5	33	31.5
		Max Energy (keV)	2.41	2.34	2.37	2.37
		Efficiency (%)	1.45	1.40	1.42	1.42
	Sphere	Range at Max Energy (μm)	65	68	69	67.33
		Max Energy (keV)	2.40	2.40	2.50	2.43
		Efficiency (%)	1.43	1.44	1.50	1.46
Sr-90	Slab	Range at Max Energy (μm)	172	177.5	216	188.5
		Max Energy (keV)	1.39	1.33	1.32	1.35
		Efficiency (%)	0.25	0.24	0.24	0.24
	Sphere	Range at Max Energy (μm)	363	387	416	388.67
		Max Energy (keV)	1.31	1.30	1.36	1.32
		Efficiency (%)	0.24	0.24	0.25	0.24
Y-90	Slab	Range at Max Energy (μm)	1147	1192	1285	1208
		Max Energy (keV)	1.01	0.96	0.93	0.97
		Efficiency (%)	0.04	0.04	0.04	0.04
	Sphere	Range at Max Energy (μm)	2004	2335	2413	2250.67
		Max Energy (keV)	0.89	0.88	0.85	0.87
		Efficiency (%)	0.04	0.04	0.04	0.04

Table 3 shows that the beta particles at high energy have a larger range than beta particles at low energy. As a result, the percentage of energy deposited in the 1 μm depletion region from beta particles with high energy is smaller than that of low energy beta particles. The same trend was observed in the transport of alpha particles in alphavoltaic systems consisting of the same geometrical setup.[24] Since most natural alpha sources have energies in the vicinity of ~5 MeV, a large range of alpha energies were not used. These results clearly show that when the range of the particle matches up with the scale length of the energy transducer, the transport efficiency increases.

3.2.2 Average beta energy calculated by 1/3 β_{max} rule

The models simulated traversing 1/3 maximum energy beta particles at 0.760 MeV emitted by an Y-90 source, at 0.182 MeV emitted by a Sr-90 source and at 0.056 MeV emitted by a S-35 source in SiC slab and sphere geometries. The energy deposited by betas at the average energy calculated by 1/3 β_{max} rule in SiC as a function of distance in the slab and sphere models is shown in Fig. 16-21. The maximum energy deposition determined by all three codes agrees well in the slab and sphere models for all three beta sources.

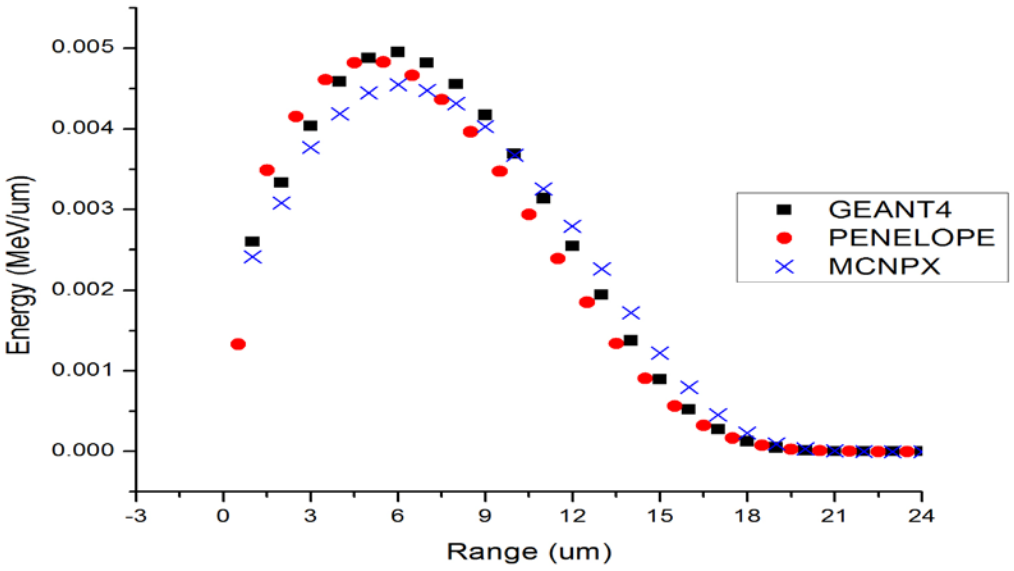

Figure 16: Simulated energy deposition of average beta energy calculated by 1/3 β_{max} rule versus distance in the slab geometry using GEANT4, PENELOPE, and MCNPX codes for S-35

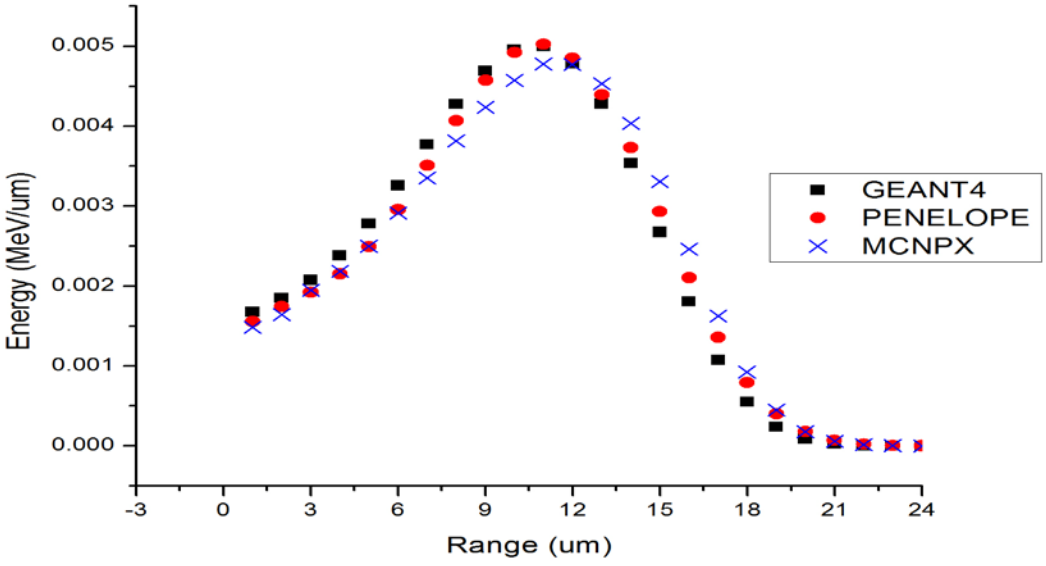

Figure 17: Simulated energy deposition of average beta energy calculated by 1/3 β_{max} rule versus distance in the sphere geometry using GEANT4, PENELOPE, and MCNPX codes for S-35

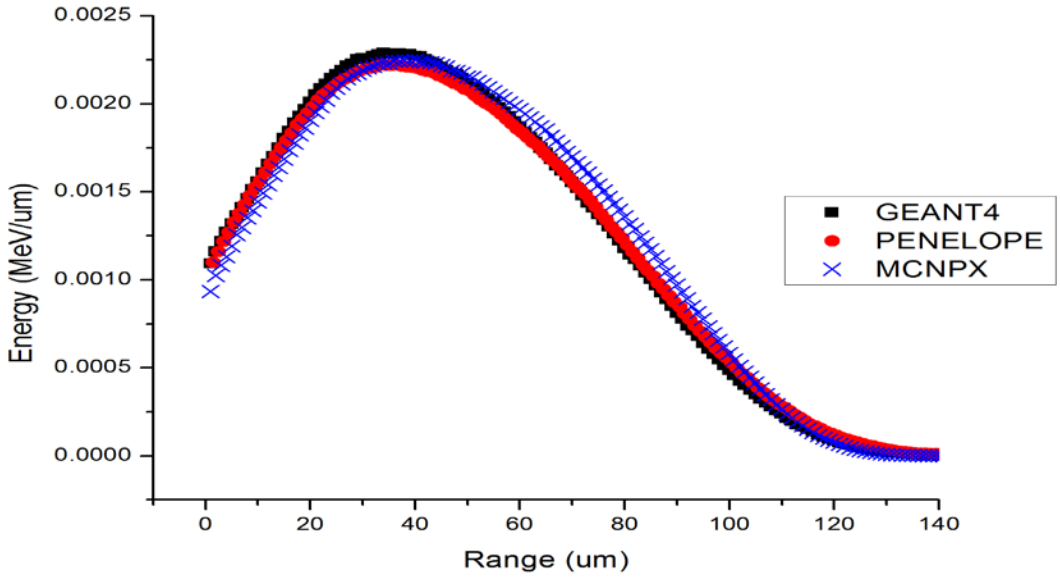

Figure 18: Simulated energy deposition of average beta energy calculated by 1/3 β_{max} rule versus distance in the slab geometry using GEANT4, PENELOPE, and MCNPX codes for Sr-90

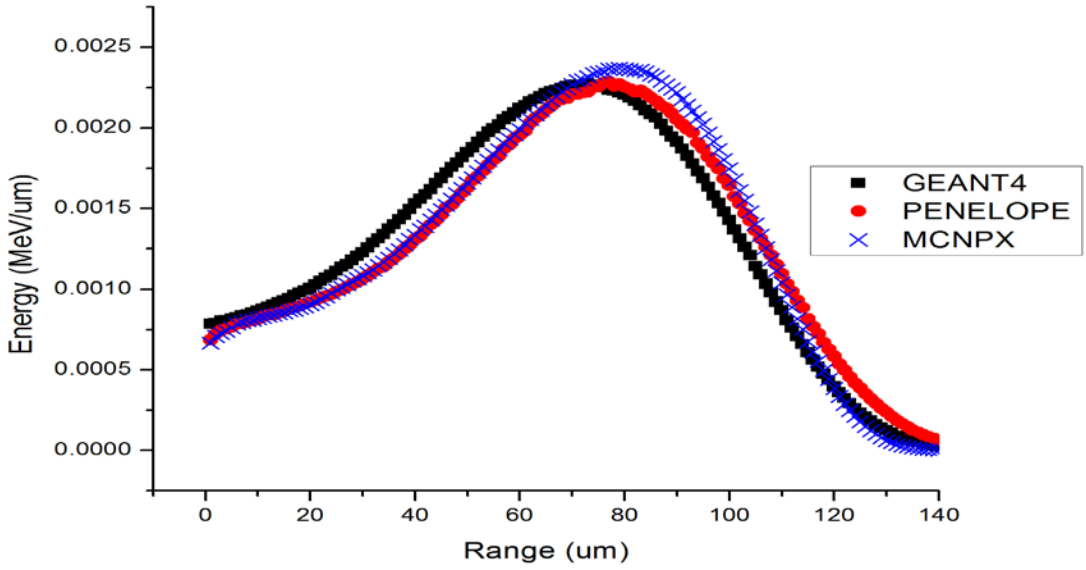

Figure 19: Simulated energy deposition of average beta energy calculated by 1/3 β_{max} rule versus distance in the sphere geometry using GEANT4, PENELOPE, and MCNPX codes for Sr-90

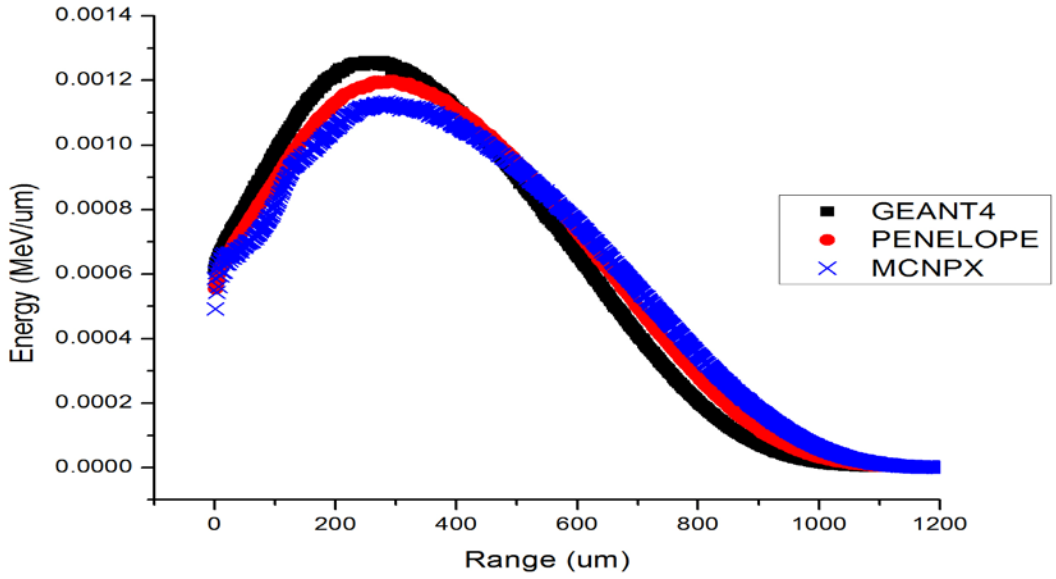

Figure 20: Simulated energy deposition of average beta energy calculated by 1/3 β_{max} rule versus distance in the slab geometry using GEANT4, PENELOPE, and MCNPX codes for Y-90

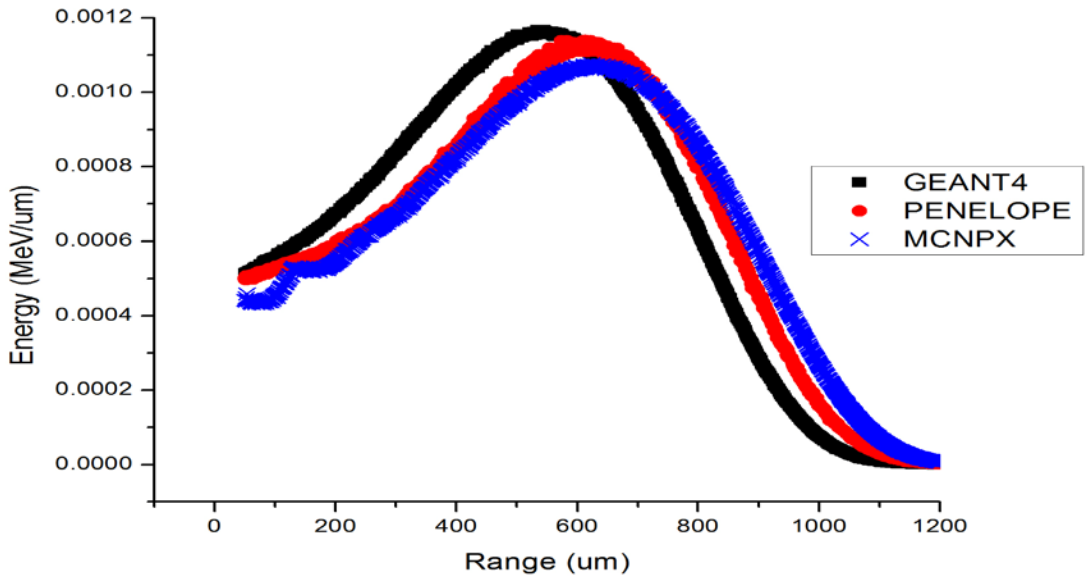

Figure 21: Simulated energy deposition of average beta energy calculated by 1/3 β_{max} rule versus distance in the sphere geometry using GEANT4, PENELOPE, and MCNPX codes for Y-90

Table 4 shows the deposited energies in the depletion zone from each model and each source. In addition, the table show that the maximum percentage of energy that is deposited in 1 μm depletion region of the SiC. The percentages of energy deposited are consistent for both the slab and the spherical models. Three codes predict that the average deposited energy efficiencies in the 1 μm thick depletion region are 8.56 % for the slab configuration and 8.85 % for the sphere configuration when using S-35 source. These values for the slab model and the sphere model using Sr-90 are 1.24 % and 1.27 %. Finally, the efficiencies using Y-90 source are 0.16 % with slab geometry and 0.15 % with sphere geometry.

Table 4: Range at which the peak energy deposition occurs, peak energy deposition, and efficiency calculations of S-35, Sr-90, and Y-90 sources with 1/3 max energy in both slab and sphere geometries using GEANT4, PENELOPE, and MCNPX codes

Source	Geometry	CONTENTS	GEANT4	PENELOPE	MCNPX	Average
S-35	Slab	Range at Max Energy (μm)	6	5.5	6	5.83
		Max Energy (keV)	4.95	4.83	4.55	4.78
		Efficiency (%)	8.87	8.66	8.15	8.56
	Sphere	Range at Max Energy (μm)	11	11	11	11
		Max Energy (keV)	5.00	5.03	4.78	4.94
		Efficiency (%)	8.96	9.01	8.57	8.85
Sr-90	Slab	Range at Max Energy (μm)	34	36.5	40	36.83
		Max Energy (keV)	2.29	2.22	2.25	2.25
		Efficiency (%)	1.26	1.22	1.24	1.24
	Sphere	Range at Max Energy (μm)	73	77	79	76.33
		Max Energy (keV)	2.28	2.29	2.37	2.31
		Efficiency (%)	1.25	1.26	1.30	1.27
Y-90	Slab	Range at Max Energy (μm)	250	295.5	285	276.83
		Max Energy (keV)	1.26	1.20	1.13	1.20
		Efficiency (%)	0.17	0.16	0.15	0.16
	Sphere	Range at Max Energy (μm)	545	613	624	594
		Max Energy (keV)	1.17	1.14	1.08	1.13
		Efficiency (%)	0.15	0.15	0.14	0.15

3.2.3 Average beta energy calculated by beta energy spectrum

The models examined the transportation of beta particles with average energies of 0.945 MeV emitted by an Y-90 source, 0.167 MeV emitted by a Sr-90 source, and 0.053 MeV emitted by a S-35 source, which were calculated by beta energy spectrum, in SiC both slab and sphere geometries. The average energies were calculated from tabulated information and generally match the 1/3 β_{max} rule except at high energy.[28] The energy deposited by betas at the average energy calculated by beta energy spectrum in SiC as a function of distance in the slab and sphere models is shown in Fig. 3. The maximum energy deposition determined by all three codes agrees well in the slab and sphere models for all three beta sources.

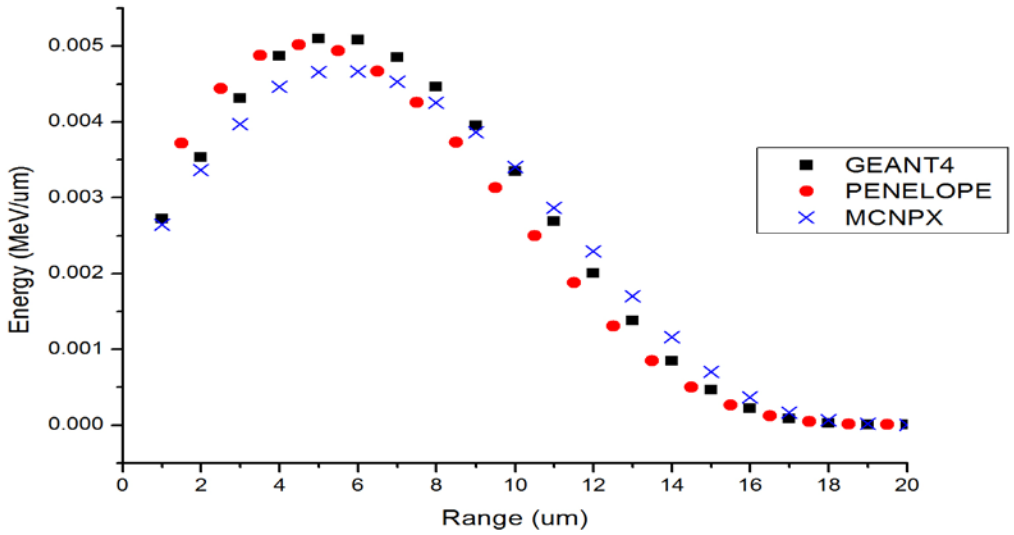

Figure 22: Simulated energy deposition of average beta energy calculated by beta energy spectrum versus distance in the slab geometry using GEANT4, PENELOPE, and MCNPX codes for S-35

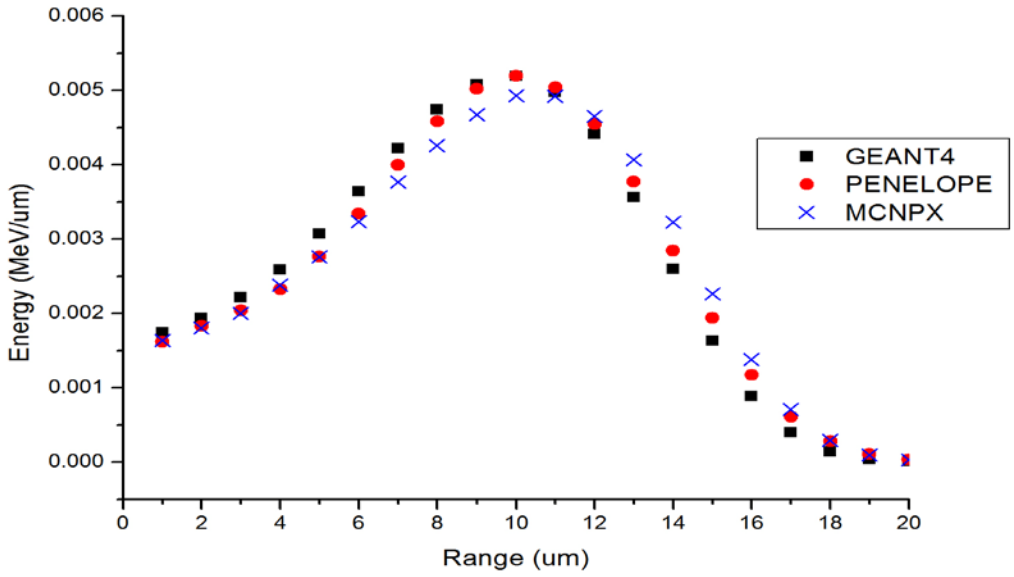

Figure 23: Simulated energy deposition of average beta energy calculated by beta energy spectrum versus distance in the sphere geometry using GEANT4, PENELOPE, and MCNPX codes for S-35

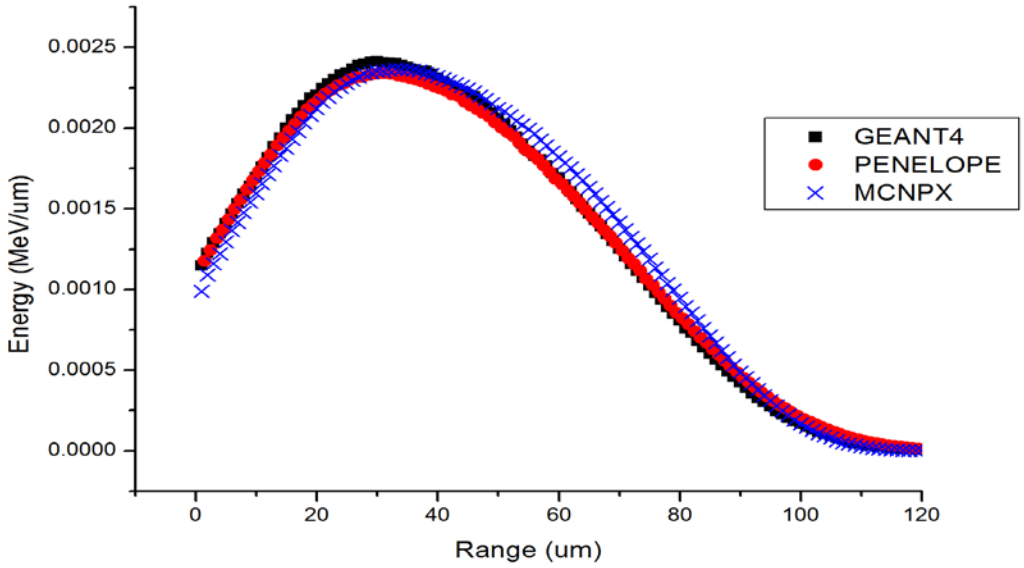

Figure 24: Simulated energy deposition of average beta energy calculated by beta energy spectrum versus distance in the slab geometry using GEANT4, PENELOPE, and MCNPX codes for Sr-90

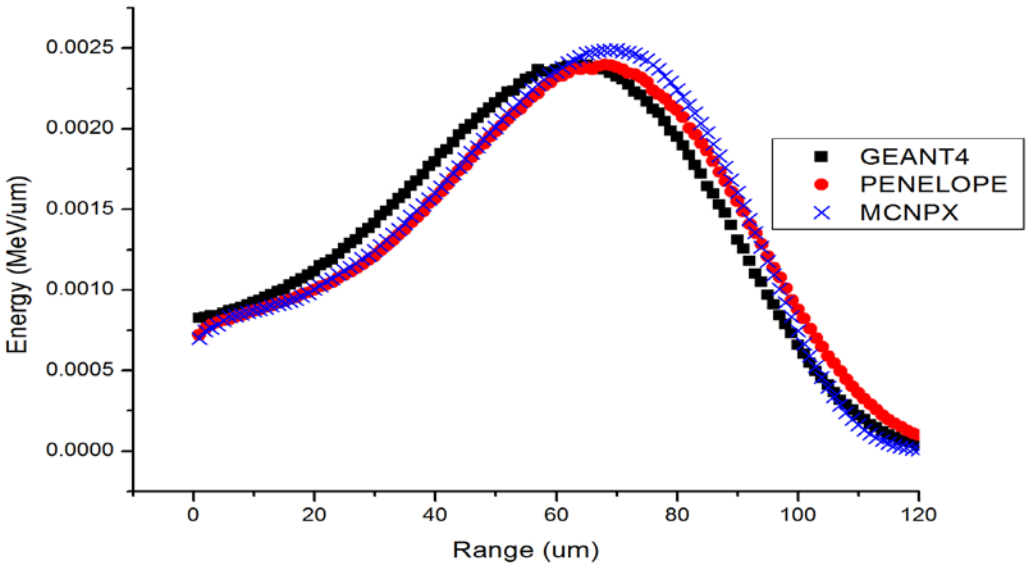

Figure 25: Simulated energy deposition of average beta energy calculated by beta energy spectrum versus distance in the sphere geometry using GEANT4, PENELOPE, and MCNPX codes for Sr-90

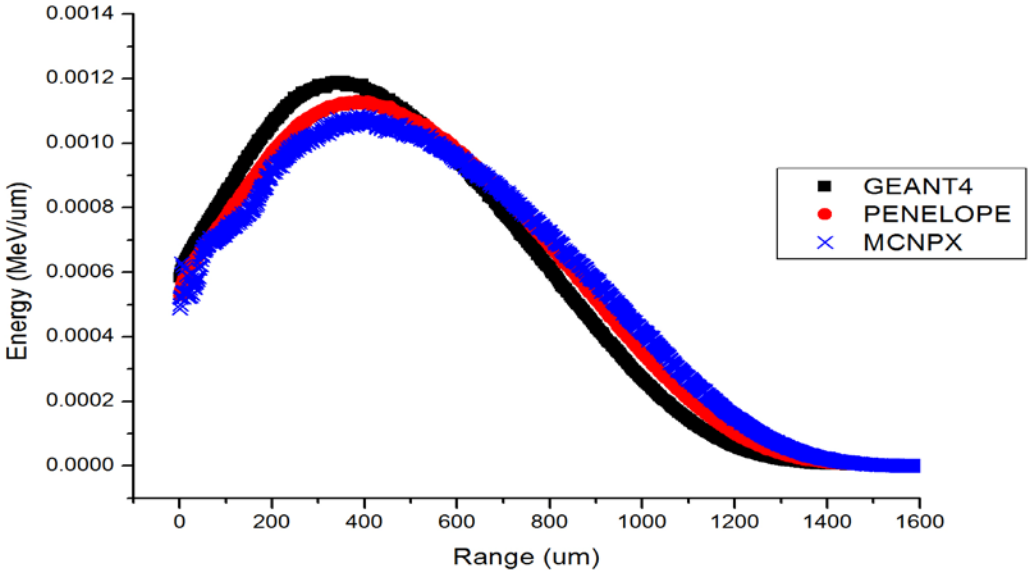

Figure 26: Simulated energy deposition of average beta energy calculated by beta energy spectrum versus distance in the slab geometry using GEANT4, PENELOPE, and MCNPX codes for Y-90

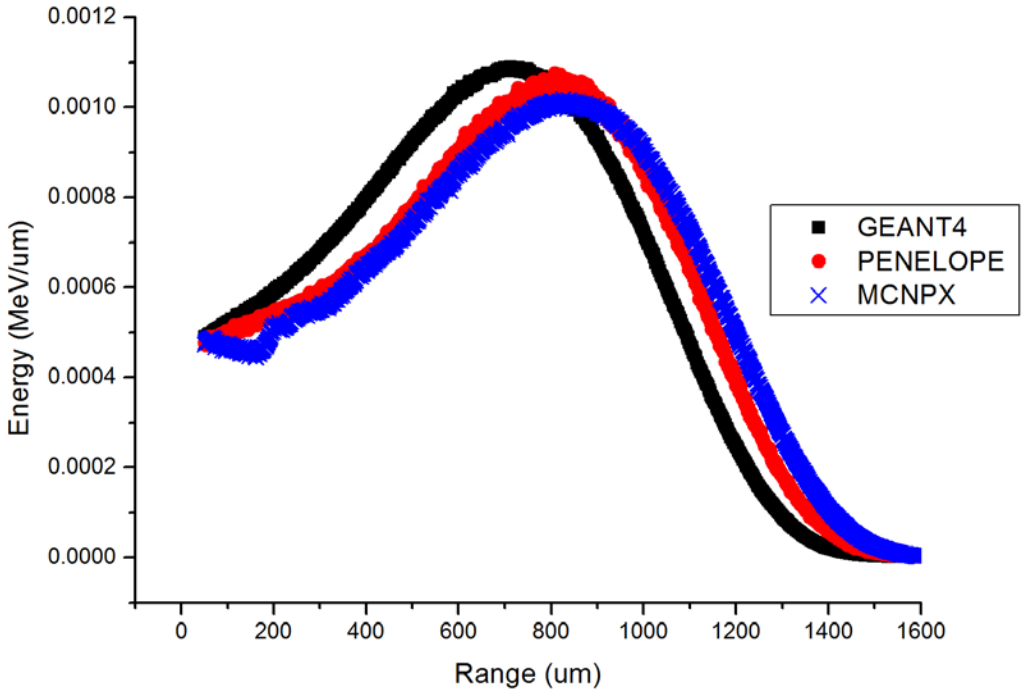

Figure 27: Simulated energy deposition of average beta energy calculated by beta energy spectrum versus distance in the sphere geometry using GEANT4, PENELOPE, and MCNPX codes for Y-90

Table 5 shows the range at which the peak energy deposition occurs, energy deposited in the depletion region, and the total fractional energy deposited in the depletion region from each model using the average mono-energetic energy from each source. The percentages of energy deposited are consistent for both the slab and the spherical models. Three codes predict that the average deposited energy in a 1 μm thick depletion region in the slab and spherical geometries is 9.28 % and 9.60 % for S-35, 1.42 % and 1.46 % for Sr-90, and 0.12% and 0.11% for Y-90, respectively.

Table 5: Range at which the peak energy deposition occurs, peak energy deposition, and efficiency calculations of S-35, Sr-90, and Y-90 sources with average energy calculate by beta energy spectrum in both slab and sphere geometries using GEANT4, PENELOPE, and MCNPX codes

Source	Geometry	CONTENTS	GEANT4	PENELOPE	MCNPX	Average
S-35	Slab	Range at Max Energy (μm)	5	4.5	6	5.2
		Max Energy (keV)	5.10	5.02	4.67	4.93
		Efficiency (%)	9.60	9.45	8.79	9.28
	Sphere	Range at Max Energy (μm)	10	10	10	10
		Max Energy (keV)	5.19	5.19	4.93	5.10
		Efficiency (%)	9.78	9.78	9.61	9.60
Sr-90	Slab	Range at Max Energy (μm)	30	31.5	33	31.5
		Max Energy (keV)	2.41	2.34	2.37	2.37
		Efficiency (%)	1.44	1.40	1.42	1.42
	Sphere	Range at Max Energy (μm)	65	68	69	67.3
		Max Energy (keV)	2.40	2.40	2.50	2.43
		Efficiency (%)	1.44	1.44	1.50	1.46
Y-90	Slab	Range at Max Energy (μm)	356	384.5	386	375.5
		Max Energy (keV)	1.19	1.13	1.09	1.14
		Efficiency (%)	0.12	0.12	0.12	0.12
	Sphere	Range at Max Energy (μm)	713	808	826	782.3
		Max Energy (keV)	1.09	1.08	1.02	1.06
		Efficiency (%)	0.12	0.11	0.11	0.11

3.2.4 Beta energy spectra

The beta particle spectra for S-35, Sr-90, and Y-90 are shown in Fig. 28-30.[29-32] Low energy sources like S-35 do not exhibit a maximum beta energy peak in their spectra, but high energy sources like Y-90 do exhibit such peaks.

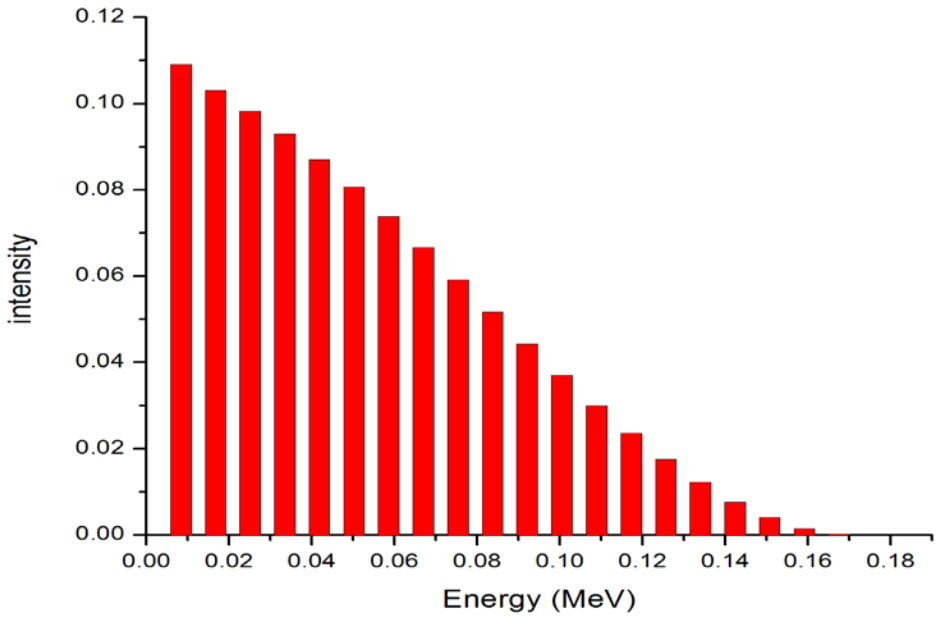

Figure 28: Beta emission energy spectra for S-35

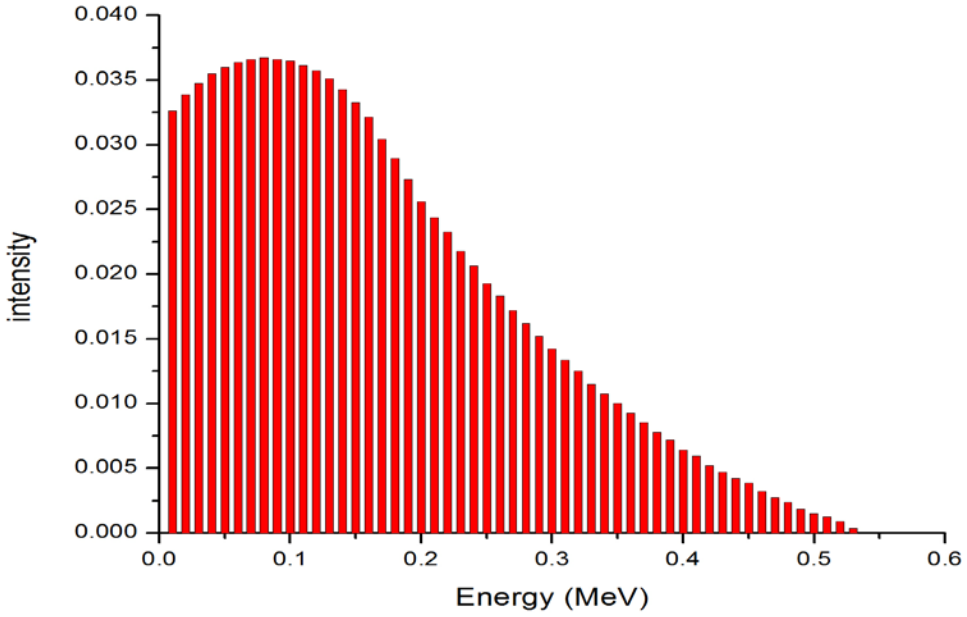

Figure 29: Beta emission energy spectra for Sr-90

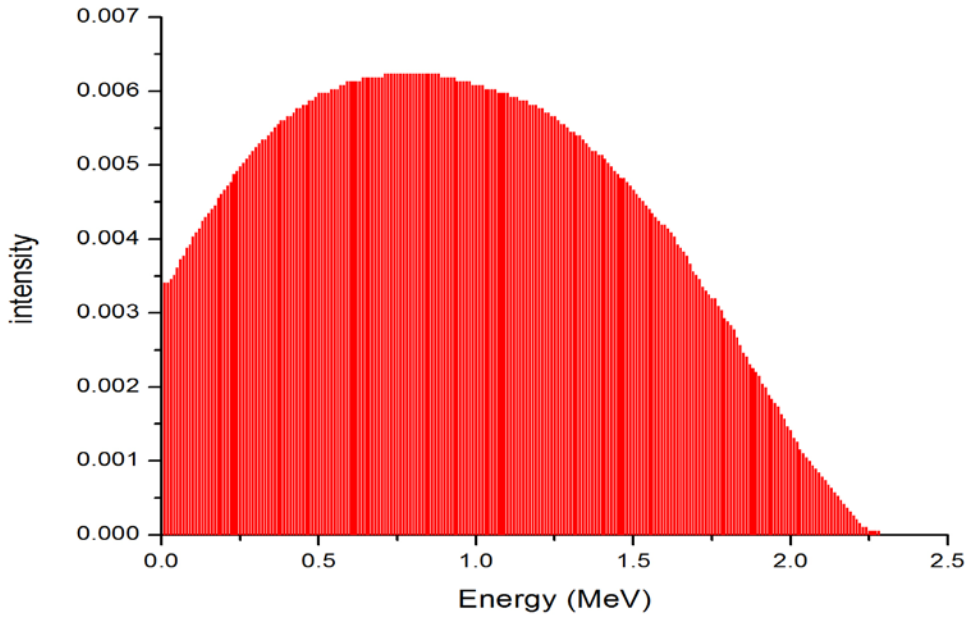

Figure 30: Beta emission energy spectra for Y-90

When simulating a beta energy spectrum source rather than a mono-energetic source, the results differ significantly. Low energy beta particles deposit more energy in the 1 µm layer than high energy beta particles because of the good match between range and transducer scale length. Figure 31-34 show that the low energy beta particles from S-35 and Sr-90 are more efficient in transporting energy to the 1 µm SiC depletion region than the high energy beta particles. In the case of Y-90, the spectra in Fig. 35-36 show that there are fewer low energy electrons so the major contributor to the energy deposition will be beta particles closer to the peak of the energy distribution. These beta particles have a poor match between range and transducer scale length which result in lower energy deposition efficiency.

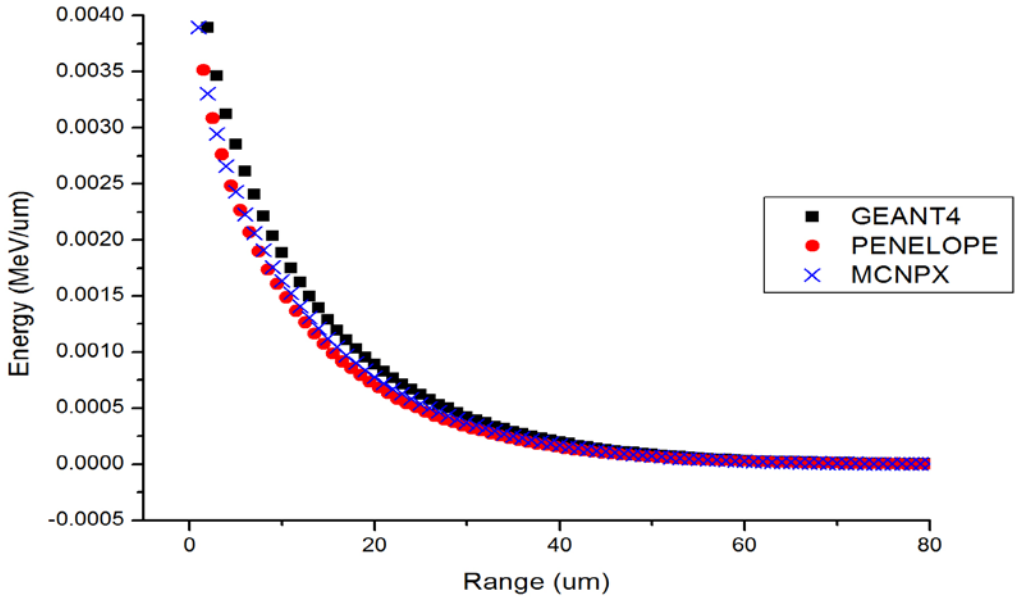

Figure 31: Simulated energy deposition by beta energy spectrum versus distance in the slab geometry using GEANT4, PENELOPE, and MCNPX codes for S-35

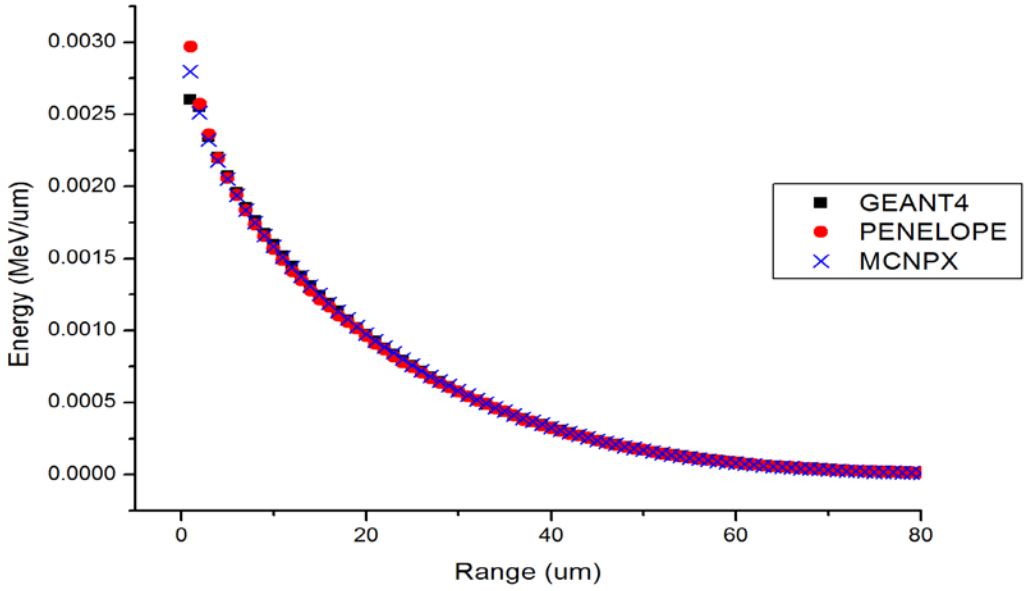

Figure 32: Simulated energy deposition by beta energy spectrum versus distance in the sphere geometry using GEANT4, PENELOPE, and MCNPX codes for S-35

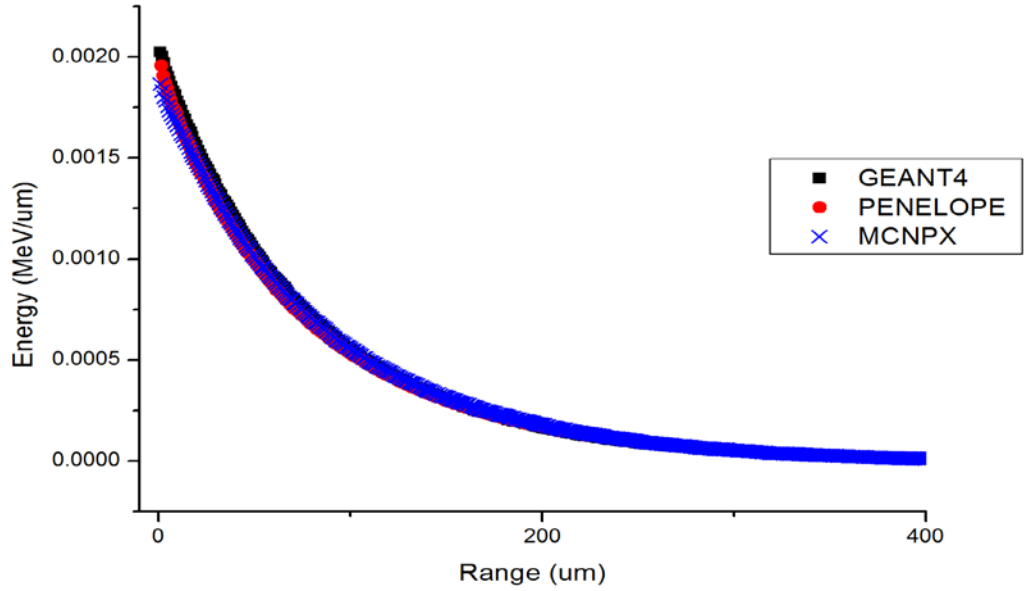

Figure 33: Simulated energy deposition by beta energy spectrum versus distance in the slab geometry using GEANT4, PENELOPE, and MCNPX codes for Sr-90

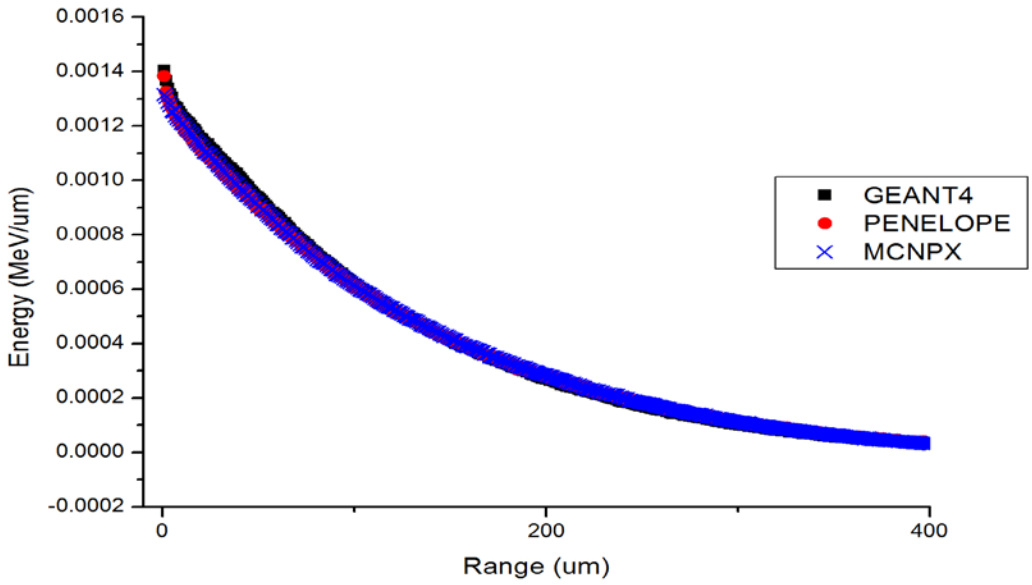

Figure 34: Simulated energy deposition by beta energy spectrum versus distance in the sphere geometry using GEANT4, PENELOPE, and MCNPX codes for Sr-90

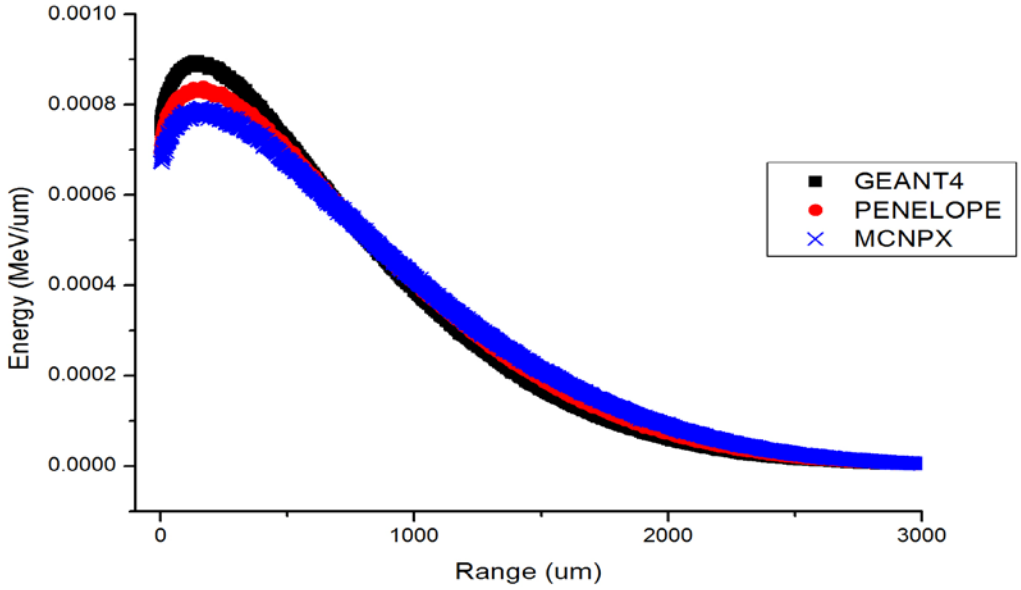

Figure 35: Simulated energy deposition by beta energy spectrum versus distance in the slab geometry using GEANT4, PENELOPE, and MCNPX codes for Y-90

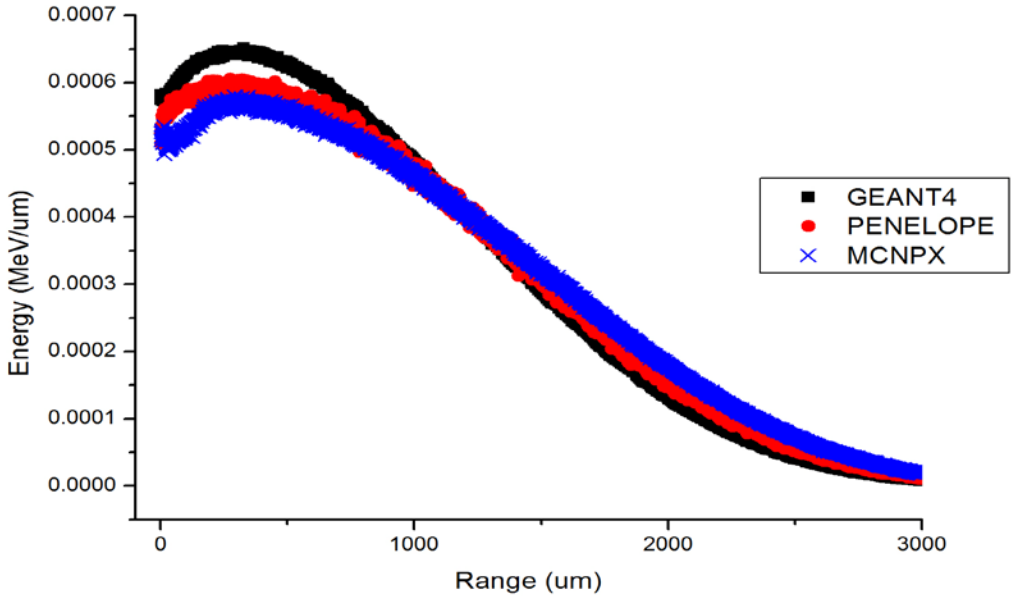

Figure 36: Simulated energy deposition by beta energy spectrum versus distance in the sphere geometry using GEANT4, PENELOPE, and MCNPX codes for Y-90

Table 6 indicates the deposited energies in the depletion region using the full beta energy spectrum. The table shows the maximum percentage of energy that is deposited in an optimally placed 1 μm depletion region in SiC. The energy deposited follows a different trend than that seen in the mono-energetic beta case. The reason for this in a full spectrum of beta energies, is that more energy is deposited near the source due to the good matchup between the range of the low energy betas and the scale length of the transducer (1 μm). The same reasoning can be used to explain the mono-energetic results. The back-scattered electrons do not deposit their energy near the source but at some distance from it. Since the betas are low in energy, the deposited energy is spread out over a larger distance and the peak of energy deposition never matches that of the slab geometry. When using the low beta energy sources such as S-35 and Sr-90, the depletion region must be placed nearer to the source to increase the efficiency. Three codes predict that the average deposited energy in an optimally placed 1 μm thick depletion region in SiC for the slab and spherical geometries is 7.32 % and 5.26 % for S-35, 1.17 % and 0.82 % for Sr-90, and 0.09 % and 0.06 % for Y-90.

Table 6: Range at which the peak energy deposition occurs, peak energy deposition, and efficiency calculations of S-35, Sr-90, and Y-90 sources with energy spectrum in both slab and sphere geometries using GEANT4, PENELOPE, and MCNPX codes

Source	Geometry	Contents	GEANT4	PENELOPE	MCNPX	Average
S-35	Slab	Range at Max Energy (μm)	1	2.5	1	1.5
		Max Energy (keV)	4.20	3.56	3.89	3.89
		Efficiency (%)	7.91	6.71	7.33	7.32
	Sphere	Range at Max Energy (μm)	1	1	1	1
		Max Energy (keV)	2.60	2.97	2.81	2.79
		Efficiency (%)	4.9	5.59	5.27	5.26
Sr-90	Slab	Range at Max Energy (μm)	1	1.5	1	1.17
		Max Energy (keV)	2.02	1.96	1.87	1.95
		Efficiency (%)	1.21	1.17	1.12	1.17
	Sphere	Range at Max Energy (μm)	1	1	1	1
		Max Energy (keV)	1.40	1.38	1.32	1.37
		Efficiency (%)	0.84	0.83	0.78	0.82
Y-90	Slab	Range at Max Energy (μm)	149	168.5	162	159.8
		Max Energy (keV)	0.90	0.84	0.79	0.84
		Efficiency (%)	0.09	0.09	0.08	0.09
	Sphere	Range at Max Energy (μm)	327	274	293	298
		Max Energy (keV)	0. 65	0.61	0.58	0.61
		Efficiency (%)	0.07	0.06	0.06	0.06

3.3. Determination of the Maximum Theoretical Efficiency

The energy absorption of radiation is a very important parameter for nuclear batteries.[22] However, the energy transport efficiency is only one part in determination of the total efficiency.[24] Assuming that the thickness of the depletion region in the semiconductor structure is about 1μm,[24] the maximum energy transport efficiency (η_d) is given in Tables 3-6 for mono-max energy, mono-1/3 max energy, mono-average energy calculated by beta energy spectrum, and poly-energy betas, respectively.

The efficiency of the betavoltaic cell (η_β) is composed of other factors. One of these factors is the pair production efficiency (η_{pp}) which is the fraction of energy deposited that goes into the production of an electron-hole pair. This is the ratio of the band-gap (E_g) of the material to the W value[33] for the solid state material.

$$\eta_{pp} = (E_g/W) \tag{6}$$

The remaining factor is the driving potential efficiency (η_{dp}), which is the ratio of the open circuit voltage (V_{oc}), to the ionization potential (E_g).

$$\eta_{dp} = (V_{oc}/E_g) \tag{7}$$

Then the efficiency of a betavoltaic is,

$$\eta_\beta = \eta_d \eta_{pp} \eta_{dp} \tag{8}$$

The theoretical maximum energy efficiency is determined by using the energy transport efficiency values calculated from the optimized slab and spherical models. For conventional betavoltaic cell structures, the isotropic source will be randomly distributed on the surface or in a volume in close proximity to the *p-n* junction. Thus the beta emitters are distributed in a way such that the bulk of the particles are not directed in the optimum direction or located at the optimum distance to the depletion region of the cell.

The sources in the slab and spherical models used in this study are optimized in both direction and distance from the depletion region. Thus, the energy transport efficiency, η_d, obtained from three codes is theoretically achievable. The pair production efficiency, η_{pp}, for SiC is 0.42.[23] The driving potential efficiency, η_{dp}, is 0.5.[6] With these values the maximum efficiency of both a slab and sphere shaped betavoltaic cells using Sr-35, Sr-90, and Y-90 beta sources with mono-energetic betas at the max beta energy,

average beta energies by 1/3 β_{max} rule and beta energy spectrum, and complete beta energy spectra are shown in Table 7.

Table 7: The maximum efficiencies obtained from calculations of three codes for mono-energetic beta particles at the max beta energy, average beta energies by 1/3 β_{max} rule and beta energy spectrum, and for the complete beta particle energy spectrum

Energy Type	Source	Model	Energy Transport Efficiency η_d(%)	Pair Production Efficiency η_{pp}	Driving Potential Efficiency η_{dp}	Maximum Efficiency η_β(%)
Max Energy	S-35	Slab	1.42	0.42	0.5	0.30
		Sphere	1.46			0.31
	Sr-90	Slab	0.24			0.05
		Sphere	0.24			0.05
	Y-90	Slab	0.04			0.008
		Sphere	0.04			0.008
1/3 Max Energy	S-35	Slab	8.56			1.80
		Sphere	8.85			1.86
	Sr-90	Slab	1.24			0.26
		Sphere	1.27			0.27
	Y-90	Slab	0.16			0.03
		Sphere	0.15			0.03
Average Energy By Energy Spectrum	S-35	Slab	9.28			1.95
		Sphere	9.60			2.02
	Sr-90	Slab	1.42			0.30
		Sphere	1.46			0.31
	Y-90	Slab	0.12			0.025
		Sphere	0.11			0.023
Energy Spectrum	S-35	Slab	7.32			1.54
		Sphere	5.26			1.10
	Sr-90	Slab	1.17			0.25
		Sphere	0.82			0.17
	Y-90	Slab	0.09			0.019
		Sphere	0.06			0.013

This study shows the best case scenario for a betavoltaic cell. As discussed, typical betavoltaic cell designs do not optimize the direction of the beta particles or the distance that the beta particles travel before stopping. Thus, a typical betavoltaic cell based on a linearly graded *p*-*n* junction will have efficiencies much less than the theoretical maximum reported here.

CHAPTER 4. CONCLUSIONS

The maximum theoretical efficiency of a linearly graded *p-n* junction based alphavoltaic cell with a typical depletion region thickness of 1 μm is approximately 2.1%. The maximum theoretical efficiencies based betavoltaic cell with a typical depletion region thickness of 1 μm are about 0.31 %, 0.05 %, and 0.008 % for the mono-energetic beta sources at the max energy of the S-35, Sr-90, and Y-90. The maximum theoretical efficiencies with same depletion region thickness are about 1.83 %, 0.27 %, and 0.03 % for the mono-energetic beta sources at the 1/3 max energy of these beta sources. The maximum theoretical are about 1.99 %, 0.31 %, and 0.02 % for the mono-energetic beta sources at the average energy of the S-35, Sr-90, and Y-90 spectra. The theoretically maximized efficiencies of these sources using the complete beta energy spectrum are approximately 1.32 %, 0.21 %, and 0.02 %.

Due to the mismatch of the scale lengths of the range for alpha and beta particles in a material and the transducer PV cell for energy conversion, the efficiency of cells will be low even in the optimized case. In terms of energy transport, alpha particles have more ideal properties when compared to beta particles. They generally follow a linear path and deposit their energy according to the Bragg curve. With these properties, alphavoltaics have the best scale length match between the particle range and the energy conversion dimensions of the PV transducer of any radiation type. Thus, alphavoltaics should have higher efficiencies than other directly interfaced radiation-based PV systems (e.g., betavoltaics).

This conclusion is significant to the field of nuclear battery technology because it presents a realistic limit to the maximum achievable efficiency of alphavoltaic and beta-voltaic cells based upon current technological limitations and provides a useful guide to understanding design issues which limit the efficiency of the cells. The match up of the scale lengths of the radiation source to the energy conversion transducer is a fundamental principle which limits the efficiency of alphavoltaic and betavoltaic cells and must be taken into account in any battery design.

BIBLIOGRAPHY

1. H. G. J. MOSELEY, "The Attainment of High Potentials by the Use of Radium," *Proc. R. Soc.London, Ser. A*, **88**, 605, 471 (1913).
2. M. A. PRELAS, E. J. CHARLSON, F. P. BOODY, and G. H. MILEY, "Advanced Nuclear Energy Conversion Using a Two Step Photon Intermediate Technique," *Prog. In Nuclear Energy*, **23,** 3, 223 (1990).
3. M. V. S. CHANDRASHEKHAR, C. I. THOMAS, H. Li, M. G. SPENCER, and A. LAL, "Demonstration of a 4H SiC betavoltaic cell," *Appl. Phys. Lett.*, **88**, 3, 033506 (2006).
4. C. D. CRESS, B. J. LANDI, R. P. RAFFAELLE, and D. M. WILT, "InGaP alpha voltaic batteries: Synthesis, modeling, and radiation tolerance," *J. Appl. Phys.*, **100**, 11, 118 (2006).
5. G. RYBICKI, C. VARGAS-ABURTO, and R. URIBE,"Silicon Carbide Alphavoltaic Battery," *Proc. 25th IEEE PV. Spec. Conf.,*Washington D.C., USA, May 13-17, 1996, IEEE Electron Devices Society (1996).
6. T. K. GHOSH, and M. A. PRELAS, *Energy Resources and Systems Volume 2: Renewable Resources*. 1st ed., Springer, New York (2011).
7. A. R. W. A. DOOLITTLE, R. AHRENKIEL, D. LEVI, G. AUGUSTINE, and R. HOPKINS, "Understanding the role of defects in limiting the minority carrier lifetime in SiC," *Mater. Res. Soc. Symp Proc.*, **483**, 197 (1997).
8. S. M. HUBBARD, M. TABIB-AZAR, S. BAILEY, G. RYBICKI, P. NEUDECK, and R. RAFFAELLE,"Effect of crystal defects on minority carrier diffusion lengths in 6H SiC," *Proc. 26th IEEE PV. Spec. Conf.*, Anaheim, CA , USA, Sep 29-Oct 03, 1997, IEEE Electron Devices Society (1997).
9. M. A. PRELAS, and K. SAHA, "Wide Band-Gap Electronics Materials," *Encylopedia of Chem. Proc.*, edited by S. Lee, CRC, 3227 (2005).
10. J.P. BIERSACK, J.F. ZIEGLER, and U. LITTMARK, *The stopping and range of ions in solids*, 1st ed., Pergamon, New York (1985).
11. C. INGUIMBERT, S. DUZELLIER, and R. ECOFFET, "Contribution of GEANT4 to the determination of sensitive volumes in case of high-integrated RAMs," *IEEE Trans. Nucl. Sci.*, **49**, 3, 1480 (2002).
12. S. AGOSTINELLI, and OTHERS, "Geant4-a simulation toolkit," *Nucl. Instrum. Methods*, **506**, 3, 250 (2003).
13. F. SALVAT, J. M. FERNANDEZ-VAREA, and J. SEMPAU, "PENELOPE-2008: A Code System for Monte Carlo Simulation of Electron and Photon Transport," *Workshop Proc.*, Barcelona, Spain, Jun 30-Jul 3, 2008, NEA-OECD (2008).
14. D. B. PELOWITZ, "MCNPX User's Manual," LA-CP-07-1473, Los Alamos National Laboratory (2008).
15. G. C. B. BEDNARZ, H. PAGANETTI, B. HAN, A. DING, and X.G. XU, "Comparison of Particle-Tracking Features in GEANT4 and MCNPX codes for Applications in Mapping of Proton Range Uncertainty," *Nucl. Technol.*, **175**, 2 (2011).
16. M. A. PRELAS, "Direct Conversion of Nuclear Energy to Electricity," *Int. Sci. J. for Alternative Energy and Ecology,* **2**, 9 (2007).

17. E. J. CHARLSON, M.A. PRELAS, E. M. CHARLSON, J. MEESE, G. POPOVICI, and T. STACY, "Diamond Photovoltaic Energy Conversion", *Proc. 2nd Int. Conf. on the Applications of Diamond Films and Related Materials*, edited by M. MURAKAWA, M. YOSHIKAWA, Y. TZENG, and W. A. YARBROUGH, MYU, Tokyo, Japan, 1993, Materials Science Monographs (1993) ; http://prelas.nuclear.missouri.edu/ne315/Lecture/NBK85.pdf (current as of June 1, 2011).
18. S. G. BAILEY, D. M. WILT, S. L. CASTRO, C. D. CRESS, and R. P. RAFFAELLE, "Photovoltaic development for alpha voltaic batteries," *Proc. 31st IEEE PV. Spec. Conf.*, Lake Buena Vista, FL, USA, Jan 3-7, 2005, The IEEE Electron Devices Society (2005).
19. F.P. BOODY, M.A. PRELAS, J.H. ANDERSON, S.J.S. NAGALINGHAM, AND G.H. MILEY "Progress in Nuclear-Pumped Lasers," *Proc. Conf. on Radiation energy conversion in space*, New York, USA, Jan 26-28, 1978, American Institute of Aeronautics and Astronautics, Inc. (1978).
20. N. A. JAMES, "Secondary Electron Production from Alpha Particles Emerging from Gold," *J. Appl. Phys.*, **34**, 3495 (1963).
21. L. L. YARGER, and J. N. ANNO, "Secondary Electron Production from Approximately 1-MeV Alpha Particles Emerging from Gold," *J. Appl. Phys.*, **37,** 2929 (1966).
22. M. A. PRELAS and H. HORA, "Radioactivity-free efficient nuclear battery, " German Patent No. DE 4300225 (A1) (07/14 1994); http://worldwide.espacenet.com/publicationDetails/biblio?DB=EPODOC&adjacent=true&locale=en_ep&FT=D&date=19940714&CC=DE&NR=4300225A1&KC=A1(current as of June 16, 2011).
23. J.D. WRBANEK, S. Y. WRBANEK, G.C. FRALICK, and L. CHEN, "Micro-Fabricated Solid-State Radiation Detectors for Active Personal Dosimetry," NASA/TM-2007-214674, National Aeronautics and Space Administration (Feb. 2007).
24. K. OH, M. A. PRELAS., R. J. SCHOTT, C. L. WEAVER, J. B. ROTHENBERGER, D. E. MONTENEGRO, E. D.LUKOSI, and D. A. WISNIEWSKI, "The Theoretical Maximum Efficiency For a Linearly Graded Alphavoltaic Nuclear Battery," *Nucl. Technol.* (2011) (submitted).
25. R. BOGUE, "Powering tomorrow's sensor: a review of technologies-Part 1," *Sensor Rev.*, **30** 3, 182 (2010).
26. C. HONSBERG, W. A. DOOLITTLE, M. ALLEN, and C. WANG,"GaN Betavoltaic Energy Converters," *Proc. 31st IEEE PV. Spec. Conf.*,Orlando, Florida, Jan 3-7, 2005, IEEE Electron Devices Society (2005).
27. D. QIAO, X. CHEN, Y. REN, and W. YUAN,"a Micro Nuclear Battery Based on SiC Schottky Barrier Diode," *J. Microelec. Mech. Sys.*,**20**, 3, 685 (2011)
28. M. G. Stabin, D. Luz, and L. C.Q.P, "Decay Data for Internal and External Dose Assessment, " Health Phys., **83**, 4, 471 (2002).
29. R. J. BUDNITZ, "Strontium-90 and Strontium-89: A Review Of Measurement Techniques Ii Environmental Media," Lawrence Berkeley Laboratory (1974).

30. L. GROSS and D. R. HAMILTON, "The Beta-Spectrum of Sulfur 35 in the Range of 0-30 Kilovolts," *Phys. Rev.*,**80**, 3, 484 (1950).
31. A. MOLJK and S. C. CURRAN, "Beta Spectra of C14 and S35" *Phys. Rev.*,**96**, 2, 395 (1954).
32. J. U. Burnham, *Radiation Protection*, N. B. Power Co., New Brunswick, Canada (1992).
33. G. FRIEDLANDER, J. W. KENNEDY, and J. M. Miller, *Nuclear and Radiocheistry*. 2nd ed., John Wiley and Sons, New York (1964)

APPENDIX A : CODE INPUTS

A. GEANT4 INPUTS (GEANT4 MULASSIS TOOL)

A.1. Po-210 alpha source in the SiC slab geometry

```
# remove the default geometry
/geometry/layer/shape slab
/geometry/material/add SiC Si-C 3.21
/geometry/layer/delete 0
# now build a new geometry
# define the layers
# format: add postion material colour_index thickness unit
/geometry/layer/add 0 SiC 1 0.001 mm
/geometry/layer/add 1 SiC 2 0.001 mm
/geometry/layer/add 2 SiC 3 0.001 mm
/geometry/layer/add 3 SiC 4 0.001 mm
/geometry/layer/add 4 SiC 1 0.001 mm
/geometry/layer/add 5 SiC 2 0.001 mm
/geometry/layer/add 6 SiC 3 0.001 mm
/geometry/layer/add 7 SiC 4 0.001 mm
/geometry/layer/add 8 SiC 1 0.001 mm
/geometry/layer/add 9 SiC 2 0.001 mm
/geometry/layer/add 10 SiC 3 0.001 mm
/geometry/layer/add 11 SiC 4 0.001 mm
/geometry/layer/add 12 SiC 1 0.001 mm
/geometry/layer/add 13 SiC 2 0.001 mm
/geometry/layer/add 14 SiC 3 0.001 mm
/geometry/layer/add 15 SiC 4 0.001 mm
/geometry/layer/add 16 SiC 1 0.001 mm
/geometry/layer/add 17 SiC 2 0.001 mm
/geometry/layer/add 18 SiC 3 0.001 mm
/geometry/layer/add 19 SiC 4 0.001 mm

# name of the CSV file for output
/analysis/file  alpha_slab

# total dose
/analysis/dose/delete 0
/analysis/dose/add 0
/analysis/dose/add 1
/analysis/dose/add 2
/analysis/dose/add 3
/analysis/dose/add 4
/analysis/dose/add 5
/analysis/dose/add 6
/analysis/dose/add 7
```

```
/analysis/dose/add 8
/analysis/dose/add 9
/analysis/dose/add 10
/analysis/dose/add 11
/analysis/dose/add 12
/analysis/dose/add 13
/analysis/dose/add 14
/analysis/dose/add 15
/analysis/dose/add 16
/analysis/dose/add 17
/analysis/dose/add 18
/analysis/dose/add 19
/analysis/dose/unit keV
/analysis/dose/list

/geometry/update

/phys/verboseLevel 1
/phys/scenario binary


# define the incident particle

/gps/particle alpha
/gps/direction 0 0 1
/gps/energy 5.307 MeV

# visulization
/event/printModulo 1000
/run/beamOn 1000000
```

A.2. Po-210 alpha source in the SiC sphere geometry

```
# remove the default geometry
/geometry/layer/shape sphere
/geometry/material/add SiC Si-C 3.21
/geometry/layer/delete 0
# now build a new geometry
# define the layers
# format: add postion material colour_index thickness unit
/geometry/layer/add   0      SiC      1     0.001  mm
/geometry/layer/add   1      SiC      2     0.001  mm
/geometry/layer/add   2      SiC      3     0.001  mm
/geometry/layer/add   3      SiC      4     0.001  mm
/geometry/layer/add   4      SiC      1     0.001  mm
/geometry/layer/add   5      SiC      2     0.001  mm
```

```
/geometry/layer/add   6      SiC      3     0.001  mm
/geometry/layer/add   7      SiC      4     0.001  mm
/geometry/layer/add   8      SiC      1     0.001  mm
/geometry/layer/add   9      SiC      2     0.001  mm
/geometry/layer/add   10     SiC      3     0.001  mm
/geometry/layer/add   11     SiC      4     0.001  mm
/geometry/layer/add   12     SiC      1     0.001  mm
/geometry/layer/add   13     SiC      2     0.001  mm
/geometry/layer/add   14     SiC      3     0.001  mm
/geometry/layer/add   15     SiC      4     0.001  mm
/geometry/layer/add   16     SiC      1     0.001  mm
/geometry/layer/add   17     SiC      2     0.001  mm
/geometry/layer/add   18     SiC      3     0.001  mm
/geometry/layer/add   19     SiC      4     0.001  mm

# name of the CSV file for output
/analysis/file  alpha_sphere

# total dose
/analysis/dose/delete 0
/analysis/dose/add 0
/analysis/dose/add 1
/analysis/dose/add 2
/analysis/dose/add 3
/analysis/dose/add 4
/analysis/dose/add 5
/analysis/dose/add 6
/analysis/dose/add 7
/analysis/dose/add 8
/analysis/dose/add 9
/analysis/dose/add 10
/analysis/dose/add 11
/analysis/dose/add 12
/analysis/dose/add 13
/analysis/dose/add 14
/analysis/dose/add 15
/analysis/dose/add 16
/analysis/dose/add 17
/analysis/dose/add 18
/analysis/dose/add 19
/analysis/dose/unit keV
/analysis/dose/list

/geometry/update

/phys/verboseLevel 1
/phys/scenario binary

# define the incident particle
```

```
/gps/particle alpha
/gps/ang/type iso
/gps/energy 5.307 MeV
/gps/position 0 0 0

# visulization
/event/printModulo 1000
/run/beamOn 1000000
```

A.3. S-35 beta source in the SiC slab geometry using 167 keV as a max energy

```
# remove the default geometry
/geometry/layer/shape slab
/geometry/material/add SiC Si1-C1 3.21
/geometry/layer/delete 0
# now build a new geometry
# define the layers
# format: add postion material colour_index thickness unit
/geometry/layer/add  0     SiC      1    0.001  mm
/geometry/layer/add  1     SiC      2    0.001  mm
/geometry/layer/add  2     SiC      3    0.001  mm
/geometry/layer/add  3     SiC      4    0.001  mm
/geometry/layer/add  4     SiC      1    0.001  mm
/geometry/layer/add  5     SiC      2    0.001  mm
/geometry/layer/add  6     SiC      3    0.001  mm
/geometry/layer/add  7     SiC      4    0.001  mm
/geometry/layer/add  8     SiC      1    0.001  mm
/geometry/layer/add  9     SiC      2    0.001  mm
/geometry/layer/add  10    SiC      3    0.001  mm
/geometry/layer/add  11    SiC      4    0.001  mm
                     ⋮
/geometry/layer/add  108     SiC      1    0.001  mm
/geometry/layer/add  109     SiC      2    0.001  mm
/geometry/layer/add  110     SiC      3    0.001  mm
/geometry/layer/add  111     SiC      4    0.001  mm
/geometry/layer/add  112     SiC      1    0.001  mm
/geometry/layer/add  113     SiC      2    0.001  mm
/geometry/layer/add  114     SiC      3    0.001  mm
/geometry/layer/add  115     SiC      4    0.001  mm
/geometry/layer/add  116     SiC      1    0.001  mm
/geometry/layer/add  117     SiC      2    0.001  mm
/geometry/layer/add  118     SiC      3    0.001  mm
/geometry/layer/add  119     SiC      4    0.001  mm

# name of the CSV file for output
```

```
/analysis/file  S35_slab_max

# total dose
/analysis/dose/delete 0
/analysis/dose/add   0
/analysis/dose/add   1
/analysis/dose/add   2
/analysis/dose/add   3
/analysis/dose/add   4
/analysis/dose/add   5
/analysis/dose/add   6
/analysis/dose/add   7
/analysis/dose/add   8
/analysis/dose/add   9
/analysis/dose/add  10
/analysis/dose/add  11
          ⋮
/analysis/dose/add  97
/analysis/dose/add  98
/analysis/dose/add  99
/analysis/dose/add  100
/analysis/dose/add  101
/analysis/dose/add  102
/analysis/dose/add  103
/analysis/dose/add  104
/analysis/dose/add  105
/analysis/dose/add  106
/analysis/dose/add  107
/analysis/dose/add  108
/analysis/dose/add  109
/analysis/dose/add  110
/analysis/dose/add  111
/analysis/dose/add  112
/analysis/dose/add  113
/analysis/dose/add  114
/analysis/dose/add  115
/analysis/dose/add  116
/analysis/dose/add  117
/analysis/dose/add  118
/analysis/dose/add  119
/analysis/dose/unit MeV
/analysis/dose/list
/geometry/update

/phys/verboseLevel 1
/phys/scenario binary

# define the incident particle
/gps/particle e-
```

```
/gps/direction 0 0 1
/gps/energy 0.167 MeV

# visulization
/event/printModulo 1000
/run/beamOn 1000000
```

A.4. S-35 beta source in the SiC sphere geometry using 55.8 keV as a 1/3 max energy

```
# remove the default geometry
/geometry/layer/shape sphere
/geometry/material/add SiC Si1-C1 3.21
/geometry/layer/delete 0
# now build a new geometry
# define the layers
# format: add postion material colour_index thickness unit
/geometry/layer/add  0     SiC      1    0.001  mm
/geometry/layer/add  1     SiC      2    0.001  mm
/geometry/layer/add  2     SiC      3    0.001  mm
/geometry/layer/add  3     SiC      4    0.001  mm
/geometry/layer/add  4     SiC      1    0.001  mm
/geometry/layer/add  5     SiC      2    0.001  mm
/geometry/layer/add  6     SiC      3    0.001  mm
/geometry/layer/add  7     SiC      4    0.001  mm
/geometry/layer/add  8     SiC      1    0.001  mm
/geometry/layer/add  9     SiC      2    0.001  mm
/geometry/layer/add  10    SiC      3    0.001  mm
/geometry/layer/add  11    SiC      4    0.001  mm
/geometry/layer/add  12    SiC      1    0.001  mm
/geometry/layer/add  13    SiC      2    0.001  mm
/geometry/layer/add  14    SiC      3    0.001  mm
/geometry/layer/add  15    SiC      4    0.001  mm
/geometry/layer/add  16    SiC      1    0.001  mm
/geometry/layer/add  17    SiC      2    0.001  mm
/geometry/layer/add  18    SiC      3    0.001  mm
/geometry/layer/add  19    SiC      4    0.001  mm
/geometry/layer/add  20    SiC      1    0.001  mm
/geometry/layer/add  21    SiC      2    0.001  mm
/geometry/layer/add  22    SiC      3    0.001  mm
/geometry/layer/add  23    SiC      4    0.001  mm

# name of the CSV file for output
/analysis/file  S35_sphere_1_3_max

# total dose
/analysis/dose/delete 0
/analysis/dose/add   0
/analysis/dose/add   1
```

```
/analysis/dose/add   2
/analysis/dose/add   3
/analysis/dose/add   4
/analysis/dose/add   5
/analysis/dose/add   6
/analysis/dose/add   7
/analysis/dose/add   8
/analysis/dose/add   9
/analysis/dose/add  10
/analysis/dose/add  11
/analysis/dose/add  12
/analysis/dose/add  13
/analysis/dose/add  14
/analysis/dose/add  15
/analysis/dose/add  16
/analysis/dose/add  17
/analysis/dose/add  18
/analysis/dose/add  19
/analysis/dose/add  20
/analysis/dose/add  21
/analysis/dose/add  22
/analysis/dose/add  23
/analysis/dose/unit MeV
/analysis/dose/list
/geometry/update

/phys/verboseLevel 1
/phys/scenario binary

# define the incident particle

/gps/particle e-
/gps/ang/type iso
/gps/energy 55.8 keV
/gps/energytype Mono
/gps/position 0 0 0

# visulization
/control/execute display.mac
/event/printModulo 1000
/run/beamOn 1000000
```

A.5. Sr-90 beta source in the SiC slab geometry using 167 keV as an average energy calculated by beta energy spectrum

```
# remove the default geometry
```

```
/geometry/layer/shape slab
/geometry/material/add SiC Si1-C1 3.21
/geometry/layer/delete 0
# now build a new geometry
# define the layers
# format: add postion material colour_index thickness unit
/geometry/layer/add   0      SiC      1     0.001  mm
/geometry/layer/add   1      SiC      2     0.001  mm
/geometry/layer/add   2      SiC      3     0.001  mm
/geometry/layer/add   3      SiC      4     0.001  mm
/geometry/layer/add   4      SiC      1     0.001  mm
/geometry/layer/add   5      SiC      2     0.001  mm
/geometry/layer/add   6      SiC      3     0.001  mm
/geometry/layer/add   7      SiC      4     0.001  mm
/geometry/layer/add   8      SiC      1     0.001  mm
/geometry/layer/add   9      SiC      2     0.001  mm
/geometry/layer/add   10     SiC      3     0.001  mm
/geometry/layer/add   11     SiC      4     0.001  mm
                      ⋮
/geometry/layer/add  108     SiC      1     0.001  mm
/geometry/layer/add  109     SiC      2     0.001  mm
/geometry/layer/add  110     SiC      3     0.001  mm
/geometry/layer/add  111     SiC      4     0.001  mm
/geometry/layer/add  112     SiC      1     0.001  mm
/geometry/layer/add  113     SiC      2     0.001  mm
/geometry/layer/add  114     SiC      3     0.001  mm
/geometry/layer/add  115     SiC      4     0.001  mm
/geometry/layer/add  116     SiC      1     0.001  mm
/geometry/layer/add  117     SiC      2     0.001  mm
/geometry/layer/add  118     SiC      3     0.001  mm
/geometry/layer/add  119     SiC      4     0.001  mm

# name of the CSV file for output
/analysis/file  Sr90_slab_avg

# total dose
/analysis/dose/delete 0
/analysis/dose/add       0
/analysis/dose/add       1
/analysis/dose/add       2
/analysis/dose/add       3
/analysis/dose/add       4
/analysis/dose/add       5
/analysis/dose/add       6
/analysis/dose/add       7
/analysis/dose/add       8
/analysis/dose/add       9
/analysis/dose/add      10
/analysis/dose/add      11
```

```
            ⋮
/analysis/dose/add     108
/analysis/dose/add     109
/analysis/dose/add     110
/analysis/dose/add     111
/analysis/dose/add     112
/analysis/dose/add     113
/analysis/dose/add     114
/analysis/dose/add     115
/analysis/dose/add     116
/analysis/dose/add     117
/analysis/dose/add     118
/analysis/dose/add     119
/analysis/dose/unit MeV
/analysis/dose/list
/geometry/update

/phys/verboseLevel 1
/phys/scenario binary

# define the incident particle
/gps/particle e-
/gps/direction 0 0 1
/gps/energy 0.167 MeV

# visulization
/control/execute display.mac
/event/printModulo 1000
/run/beamOn 1000000
```

A.6. Sr-90 beta source in the SiC sphere geometry using beta energy spectra

```
# remove the default geometry
/geometry/layer/shape sphere
/geometry/material/add SiC Si1-C1 3.21
/geometry/layer/delete 0
# now build a new geometry
# define the layers
# format: add postion material colour_index thickness unit
 /geometry/layer/add   0      SiC      1     0.001  mm
/geometry/layer/add   1      SiC      2     0.001  mm
/geometry/layer/add   2      SiC      3     0.001  mm
/geometry/layer/add   3      SiC      4     0.001  mm
/geometry/layer/add   4      SiC      1     0.001  mm
/geometry/layer/add   5      SiC      2     0.001  mm
/geometry/layer/add   6      SiC      3     0.001  mm
```

```
/geometry/layer/add   7      SiC      4     0.001  mm
/geometry/layer/add   8      SiC      1     0.001  mm
/geometry/layer/add   9      SiC      2     0.001  mm
/geometry/layer/add   10     SiC      3     0.001  mm
/geometry/layer/add   11     SiC      4     0.001  mm
                      ⋮
/geometry/layer/add  388     SiC      1     0.001  mm
/geometry/layer/add  389     SiC      2     0.001  mm
/geometry/layer/add  390     SiC      3     0.001  mm
/geometry/layer/add  391     SiC      4     0.001  mm
/geometry/layer/add  392     SiC      1     0.001  mm
/geometry/layer/add  393     SiC      2     0.001  mm
/geometry/layer/add  394     SiC      3     0.001  mm
/geometry/layer/add  395     SiC      4     0.001  mm
/geometry/layer/add  396     SiC      1     0.001  mm
/geometry/layer/add  397     SiC      2     0.001  mm
/geometry/layer/add  398     SiC      3     0.001  mm
/geometry/layer/add  399     SiC      4     0.001  mm

# name of the CSV file for output
/analysis/file  Sr90_sphere_spectra

# total dose
/analysis/dose/delete 0
/analysis/dose/add       0
/analysis/dose/add       1
/analysis/dose/add       2
/analysis/dose/add       3
/analysis/dose/add       4
/analysis/dose/add       5
/analysis/dose/add       6
/analysis/dose/add       7
/analysis/dose/add       8
/analysis/dose/add       9
/analysis/dose/add      10
/analysis/dose/add      11
             ⋮
/analysis/dose/add     388
/analysis/dose/add     389
/analysis/dose/add     390
/analysis/dose/add     391
/analysis/dose/add     392
/analysis/dose/add     393
/analysis/dose/add     394
/analysis/dose/add     395
/analysis/dose/add     396
/analysis/dose/add     397
/analysis/dose/add     398
/analysis/dose/add     399
```

```
/analysis/dose/unit MeV
/analysis/dose/list

/geometry/update

/phys/verboseLevel 1
/phys/scenario binary


# define the incident particle
/gps/particle e-
/gps/ang/type iso
/gps/position 0 0 0
/gps/ene/type Arb
/gps/hist/type arb
/gps/histpoint     0               0
/gps/histpoint  0.01      0.03264095
/gps/histpoint  0.02     0.033877349
/gps/histpoint  0.03     0.034742829
/gps/histpoint  0.04     0.035484669
/gps/histpoint  0.05     0.035979228
/gps/histpoint  0.06     0.036350148
/gps/histpoint  0.07     0.036597428
/gps/histpoint  0.08     0.036721068
/gps/histpoint  0.09     0.036597428
/gps/histpoint   0.1     0.036473788
/gps/histpoint  0.11     0.036102868
/gps/histpoint  0.12     0.035731949
/gps/histpoint  0.13     0.035113749
/gps/histpoint  0.14     0.034248269
/gps/histpoint  0.15     0.033259149
/gps/histpoint  0.16      0.03214639
/gps/histpoint  0.17      0.03041543
/gps/histpoint  0.18     0.028931751
/gps/histpoint  0.19     0.027324431
/gps/histpoint   0.2     0.025593472
/gps/histpoint  0.21     0.024357072
/gps/histpoint  0.22     0.023244313
/gps/histpoint  0.23     0.021760633
/gps/histpoint  0.24     0.020647873
/gps/histpoint  0.25     0.019287834
/gps/histpoint  0.26     0.018298714
/gps/histpoint  0.27     0.017185955
/gps/histpoint  0.28     0.016196835
/gps/histpoint  0.29     0.015207715
/gps/histpoint   0.3     0.014218595
/gps/histpoint  0.31     0.013353116
/gps/histpoint  0.32     0.012487636
/gps/histpoint  0.33     0.011498516
```

```
/gps/histpoint  0.34     0.010756677
/gps/histpoint  0.35     0.010014837
/gps/histpoint  0.36     0.009272997
/gps/histpoint  0.37     0.008531157
/gps/histpoint  0.38     0.007789318
/gps/histpoint  0.39     0.007171118
/gps/histpoint   0.4     0.006429278
/gps/histpoint  0.41     0.005934718
/gps/histpoint  0.42     0.005192878
/gps/histpoint  0.43     0.004698318
/gps/histpoint  0.44     0.004203759
/gps/histpoint  0.45     0.003832839
/gps/histpoint  0.46     0.003214639
/gps/histpoint  0.47     0.002720079
/gps/histpoint  0.48     0.002349159
/gps/histpoint  0.49     0.001854599
/gps/histpoint   0.5      0.00148368
/gps/histpoint  0.51       0.0012364
/gps/histpoint  0.52      0.00086548
/gps/histpoint  0.53      0.00037092
/gps/histpoint  0.54               0
/gps/histpoint  0.55               0
/gps/hist/inter Lin

# visulization
/event/printModulo 1000
/run/beamOn 1000000
```

B. PENELOPE INPUTS

B.1. S-35 beta source in the SiC slab geometry using 167 keV as a max energy using pencyl

```
TITLE  Electron beam on an Silicon Carbide slab
       .
GSTART >>>>>>>> Beginning of the geometry definition list.
LAYER        0.00 +0.01  1
CENTRE       0.00  0.00
CYLIND   1   0.00  1000.00
LAYER        0.01 +0.02  2
CENTRE       0.00  0.00
CYLIND   1   0.00  1000.00
GEND   <<<<<<<< End of the geometry definition list.
       .
```

```
       >>>>>>>> Source definition.
SKPAR  1   [Primary particles: 1=electron, 2=photon, 3=positron]
SENERG 167.e3       [Initial energy (monoenergetic sources only)]
SPOSIT 0 0 0                   [Coordinates of the source centre]
SCONE  0 0 0                        [Conical beam; angles in deg]
       .
       >>>>>>>> Material data and simulation parameters.
MFNAME SiC.mat                     [Material file, up to 20 chars]
       .
       >>>>>>>> Dose and charge distributions.
DOSE2D 1 1 100 100[Tally 2D dose and charge dists. in body KL,KC]
DOSE2D 2 1 100 100[Tally 2D dose and charge dists. in body KL,KC]
       .
       >>>>>>>> Job properties
NSIMSH 1000000              [Desired number of simulated showers]
       .
END                              [Ends the reading of input data]
```

B.2. S-35 beta source in the SiC sphere geometry using 55.8 keV as a 1/3 max energy using penmain

```
TITLE  S-35 beta source in the SiC sphere geometry
       .
       >>>>>>>> Source definition.
SKPAR  1    [Primary particles: 1=electron, 2=photon, 3=positron]
SENERG 55800        [Initial energy (monoenergetic sources only)]
SPOSIT 0 0 0                          [Coordinates of the source]
SCONE  0 0 180.0                   [Conical beam; angles in deg]
       .
       >>>>>>>> Material data and simulation parameters.
MFNAME SiC.mat                     [Material file, up to 20 chars]
       .
       >>>>>>>> Geometry definition file.
GEOMFN S35_sphere_1_3_max.geo     [Geometry file, up to 20 chars]
       .
       >>>>>>>> Job properties
RESUME dump.dmp            [Resume from this dump file, 20 chars]
DUMPTO dump.dmp               [Generate this dump file, 20 chars]
DUMPP  60                                  [Dumping period, in sec]
       .
NSIMSH 1000000              [Desired number of simulated showers]
TIME   1000000                 [Allotted simulation time, in sec]
       .
END                              [Ends the reading of input data]
```

B.3. Sr-90 beta source in the SiC sphere geometry using beta energy spectra using penmain

```
TITLE  Sr-90 beta source in the SiC sphere geometry
       .
       >>>>>>>> Source definition.
SKPAR  1    [Primary particles: 1=electron, 2=photon, 3=positron]
       .
       Energy spectrum of beta rays from Sr-90...
SPECTR   0.00000E+00  3.26410E-02
SPECTR   1.00000E+04  3.38773E-02
SPECTR   2.00000E+04  3.47428E-02
SPECTR   3.00000E+04  3.54847E-02
SPECTR   4.00000E+04  3.59792E-02
SPECTR   5.00000E+04  3.63501E-02
SPECTR   6.00000E+04  3.65974E-02
SPECTR   7.00000E+04  3.67211E-02
SPECTR   8.00000E+04  3.65974E-02
SPECTR   9.00000E+04  3.64738E-02
SPECTR   1.00000E+05  3.61029E-02
SPECTR   1.10000E+05  3.57319E-02
SPECTR   1.20000E+05  3.51137E-02
SPECTR   1.30000E+05  3.42483E-02
SPECTR   1.40000E+05  3.32591E-02
SPECTR   1.50000E+05  3.21464E-02
SPECTR   1.60000E+05  3.04154E-02
SPECTR   1.70000E+05  2.89318E-02
SPECTR   1.80000E+05  2.73244E-02
SPECTR   1.90000E+05  2.55935E-02
SPECTR   2.00000E+05  2.43571E-02
SPECTR   2.10000E+05  2.32443E-02
SPECTR   2.20000E+05  2.17606E-02
SPECTR   2.30000E+05  2.06479E-02
SPECTR   2.40000E+05  1.92878E-02
SPECTR   2.50000E+05  1.82987E-02
SPECTR   2.60000E+05  1.71860E-02
SPECTR   2.70000E+05  1.61968E-02
SPECTR   2.80000E+05  1.52077E-02
SPECTR   2.90000E+05  1.42186E-02
SPECTR   3.00000E+05  1.33531E-02
SPECTR   3.10000E+05  1.24876E-02
SPECTR   3.20000E+05  1.14985E-02
SPECTR   3.30000E+05  1.07567E-02
SPECTR   3.40000E+05  1.00148E-02
SPECTR   3.50000E+05  9.27300E-03
SPECTR   3.60000E+05  8.53116E-03
SPECTR   3.70000E+05  7.78932E-03
SPECTR   3.80000E+05  7.17112E-03
```

```
SPECTR   3.90000E+05  6.42928E-03
SPECTR   4.00000E+05  5.93472E-03
SPECTR   4.10000E+05  5.19288E-03
SPECTR   4.20000E+05  4.69832E-03
SPECTR   4.30000E+05  4.20376E-03
SPECTR   4.40000E+05  3.83284E-03
SPECTR   4.50000E+05  3.21464E-03
SPECTR   4.60000E+05  2.72008E-03
SPECTR   4.70000E+05  2.34916E-03
SPECTR   4.80000E+05  1.85460E-03
SPECTR   4.90000E+05  1.48368E-03
SPECTR   5.00000E+05  1.23640E-03
SPECTR   5.10000E+05  8.65480E-04
SPECTR   5.20000E+05  3.70920E-04
SPECTR   5.30000E+05  0.00000E+00
       .
SPOSIT 0 0 0                          [Coordinates of the source]
SCONE  0 0 180.0                    [Conical beam; angles in deg]
       .
       >>>>>>>> Material data and simulation parameters.
MFNAME SiC.mat                    [Material file, up to 20 chars]
       .
       >>>>>>>> Geometry definition file.
GEOMFN Sr90_sphere_spectra.geo
       .
       >>>>>>>> Job properties
RESUME dump.dmp            [Resume from this dump file, 20 chars]
DUMPTO dump.dmp               [Generate this dump file, 20 chars]
DUMPP  60                                [Dumping period, in sec]
       .
NSIMSH 1000000              [Desired number of simulated showers]
TIME   1000000                 [Allotted simulation time, in sec]
       .
END                              [Ends the reading of input data]
```

C. MCNPX INPUTS

C.1. S-35 beta source in the SiC slab geometry using 167 keV as a max energy

```
SiC slab with S-35 beta source
c Cell Card
1       1   -3.21    -1
2       1   -3.21 1  -2
3       1   -3.21 2  -3
4       1   -3.21 3  -4
5       1   -3.21 4  -5
6       1   -3.21 5  -6
```

```
7       1   -3.21 6  -7
8       1   -3.21 7  -8
9       1   -3.21 8  -9
10      1   -3.21 9  -10
              ⋮
111     1   -3.21 110 -111
112     1   -3.21 111 -112
113     1   -3.21 112 -113
114     1   -3.21 113 -114
115     1   -3.21 114 -115
116     1   -3.21 115 -116
117     1   -3.21 116 -117
118     1   -3.21 117 -118
119     1   -3.21 118 -119
120     1   -3.21 119 -120
121     0         120 -121
122     0         121

c Surface Card
1       RCC   0     0     0     0     0       0.0001  1000
2       RCC   0     0     0     0     0       0.0002  1000
3       RCC   0     0     0     0     0       0.0003  1000
4       RCC   0     0     0     0     0       0.0004  1000
5       RCC   0     0     0     0     0       0.0005  1000
6       RCC   0     0     0     0     0       0.0006  1000
7       RCC   0     0     0     0     0       0.0007  1000
8       RCC   0     0     0     0     0       0.0008  1000
9       RCC   0     0     0     0     0       0.0009  1000
10      RCC   0     0     0     0     0       0.001   1000
                              ⋮
111     RCC   0     0     0     0     0       0.0111  1000
112     RCC   0     0     0     0     0       0.0112  1000
113     RCC   0     0     0     0     0       0.0113  1000
114     RCC   0     0     0     0     0       0.0114  1000
115     RCC   0     0     0     0     0       0.0115  1000
116     RCC   0     0     0     0     0       0.0116  1000
117     RCC   0     0     0     0     0       0.0117  1000
118     RCC   0     0     0     0     0       0.0118  1000
119     RCC   0     0     0     0     0       0.0119  1000
120     RCC   0     0     0     0     0       0.012   1000
121     RCC   0     0     0     0     0       1       1000

c Mode card
MODE e
c
c
c Materials
m1    14000.03e          -0.70045   $ MAT1
      6000.03e           -0.299548  $ SiC
```

```
c
IMP:e 1 119r 0 1r
c
c
c Source Definition
sdef PAR=e  DIR=1   POS=0 0 0   VEC=0 0 1   ERG=0.167
c
c Tallies
F6:e 1  2  3  4  5  6  7  8  9  10$
     11 12 13 14 15 16 17 18 19 20$
     21 22 23 24 25 26 27 28 29 30$
     31 32 33 34 35 36 37 38 39 40$
     41 42 43 44 45 46 47 48 49 50$
     51 52 53 54 55 56 57 58 59 60$
     61 62 63 64 65 66 67 68 69 70$
     71 72 73 74 75 76 77 78 79 80$
     81 82 83 84 85 86 87 88 89 90$
     91 92 93 94 95 96 97 98 99 100$
     101 102 103 104 105 106 107 108 109 110$
     111 112 113 114 115 116 117 118 119 120$
     T
SD6  1  1  1  1  1  1  1  1  1  1$
     1  1  1  1  1  1  1  1  1  1$
     1  1  1  1  1  1  1  1  1  1$
     1  1  1  1  1  1  1  1  1  1$
     1  1  1  1  1  1  1  1  1  1$
     1  1  1  1  1  1  1  1  1  1$
     1  1  1  1  1  1  1  1  1  1$
     1  1  1  1  1  1  1  1  1  1$
     1  1  1  1  1  1  1  1  1  1$
     1  1  1  1  1  1  1  1  1  1$
     1  1  1  1  1  1  1  1  1  1$
     1
c
nps 1E06
c
print
```

C.2. S-35 beta source in the SiC sphere geometry using 55.8 keV as a 1/3 max energy

```
SiC Sphere with S-35 beta source at center
c Cell Card
1       1   -3.21    -1
2       1   -3.21 1  -2
3       1   -3.21 2  -3
4       1   -3.21 3  -4
5       1   -3.21 4  -5
```

```
6       1   -3.21 5  -6
7       1   -3.21 6  -7
8       1   -3.21 7  -8
9       1   -3.21 8  -9
10      1   -3.21 9  -10
11      1   -3.21 10 -11
12      1   -3.21 11 -12
13      1   -3.21 12 -13
14      1   -3.21 13 -14
15      1   -3.21 14 -15
16      1   -3.21 15 -16
17      1   -3.21 16 -17
18      1   -3.21 17 -18
19      1   -3.21 18 -19
20      1   -3.21 19 -20
21      1   -3.21 20 -21
22      1   -3.21 21 -22
23      1   -3.21 22 -23
24      1   -3.21 23 -24
25      0         24 -25
26      0         25

c Surface Card
1         so 0.0001
2         so 0.0002
3         so 0.0003
4         so 0.0004
5         so 0.0005
6         so 0.0006
7         so 0.0007
8         so 0.0008
9         so 0.0009
10        so 0.0010
11        so 0.0011
12        so 0.0012
13        so 0.0013
14        so 0.0014
15        so 0.0015
16        so 0.0016
17        so 0.0017
18        so 0.0018
19        so 0.0019
20        so 0.0020
21        so 0.0021
22        so 0.0022
23        so 0.0023
24        so 0.0024
25        so 1
```

```
c Mode card
MODE e
c
c
c Materials
m1    14000.03e          -0.70045   $ MAT1
      6000.03e           -0.299548  $ SiC
c
IMP:e 1 23r 0 1r
c
c Source Definition
sdef PAR=e  ERG=0.0558
c
c Tallies
F6:e 1  2  3  4  5  6  7  8  9  10$
     11 12 13 14 15 16 17 18 19 20$
     21 22 23 24
     T
SD6  1  1  1  1  1  1  1  1  1  1$
     1  1  1  1  1  1  1  1  1  1$
     1  1  1  1  1
c
nps 1E06
c
print
```

C.3. Sr-90 beta source in the SiC slab geometry using beta energy spectra

```
Sr-90 beta source in the SiC slab geometry c Cell Card
1       1   -3.21    -1
2       1   -3.21 1  -2
3       1   -3.21 2  -3
4       1   -3.21 3  -4
5       1   -3.21 4  -5
6       1   -3.21 5  -6
7       1   -3.21 6  -7
8       1   -3.21 7  -8
9       1   -3.21 8  -9
10      1   -3.21 9  -10
                  ⋮
391      1   -3.21 390 -391
392      1   -3.21 391  -392
393      1   -3.21 392  -393
394      1   -3.21 393  -394
395      1   -3.21 394  -395
396      1   -3.21 395  -396
397      1   -3.21 396  -397
398      1   -3.21 397  -398
```

```
399      1   -3.21 398  -399
400      1   -3.21 399  -400
401      0         400  -401  $ Void
402      0         401       $ Void

c Surface Card
1       RCC   0     0     0     0     0       0.0001  1000
2       RCC   0     0     0     0     0       0.0002  1000
3       RCC   0     0     0     0     0       0.0003  1000
4       RCC   0     0     0     0     0       0.0004  1000
5       RCC   0     0     0     0     0       0.0005  1000
6       RCC   0     0     0     0     0       0.0006  1000
7       RCC   0     0     0     0     0       0.0007  1000
8       RCC   0     0     0     0     0       0.0008  1000
9       RCC   0     0     0     0     0       0.0009  1000
10      RCC   0     0     0     0     0       0.001   1000
                          ⋮
391     RCC   0     0     0     0     0       0.0391  1000
392     RCC   0     0     0     0     0       0.0392  1000
393     RCC   0     0     0     0     0       0.0393  1000
394     RCC   0     0     0     0     0       0.0394  1000
395     RCC   0     0     0     0     0       0.0395  1000
396     RCC   0     0     0     0     0       0.0396  1000
397     RCC   0     0     0     0     0       0.0397  1000
398     RCC   0     0     0     0     0       0.0398  1000
399     RCC   0     0     0     0     0       0.0399  1000
400     RCC   0     0     0     0     0       0.04    1000
401     RCC   0     0     0     0     0       1       1000

c Mode card
MODE e
c
c
c Materials
m1    14000.03e          -0.70045   $ MAT1
      6000.03e           -0.299548  $ SiC
c
IMP:e 1 399r 0 1r
c
c Source Definition
sdef PAR=e  DIR=1   POS=0 0 0   VEC=0 0 1   ERG=d1
si1  h 0 54i 0.55
sp1  00.03264095 0.033877349 0.034742829 0.035484669 0.035979228
     0.036350148 0.036597428 0.036721068 0.036597428 0.036473788
     0.036102868 0.035731949 0.035113749 0.034248269 0.033259149
     0.03214639  0.03041543  0.028931751 0.027324431 0.025593472
     0.024357072 0.023244313 0.021760633 0.020647873 0.019287834
     0.018298714 0.017185955 0.016196835 0.015207715  0.014218595
     0.013353116 0.012487636 0.011498516 0.010756677 0.010014837
```

```
     0.009272997 0.008531157 0.007789318 0.007171118 0.006429278
     0.005934718 0.005192878 0.004698318 0.004203759 0.003832839
     0.003214639 0.002720079 0.002349159 0.001854599 0.00148368
     0.0012364   0.00086548  0.00037092  0           0
c
c Tallies
F6:e 1  2  3  4  5  6  7  8  9  10$
     11 12 13 14 15 16 17 18 19 20$
     21 22 23 24 25 26 27 28 29 30$
     31 32 33 34 35 36 37 38 39 40$
     41 42 43 44 45 46 47 48 49 50$
     51 52 53 54 55 56 57 58 59 60$
     61 62 63 64 65 66 67 68 69 70$
     71 72 73 74 75 76 77 78 79 80$
     81 82 83 84 85 86 87 88 89 90$
     91 92 93 94 95 96 97 98 99 100$
     101 102 103 104 105 106 107 108 109 110$
     111 112 113 114 115 116 117 118 119 120$
     121 122 123 124 125 126 127 128 129 130$
     131 132 133 134 135 136 137 138 139 140$
     141 142 143 144 145 146 147 148 149 150$
     151 152 153 154 155 156 157 158 159 160$
     161 162 163 164 165 166 167 168 169 170$
     171 172 173 174 175 176 177 178 179 180$
     181 182 183 184 185 186 187 188 189 190$
     191 192 193 194 195 196 197 198 199 200$
     201 202 203 204 205 206 207 208 209 210$
     211 212 213 214 215 216 217 218 219 220$
     221 222 223 224 225 226 227 228 229 230$
     231 232 233 234 235 236 237 238 239 240$
     241 242 243 244 245 246 247 248 249 250$
     251 252 253 254 255 256 257 258 259 260$
     261 262 263 264 265 266 267 268 269 270$
     271 272 273 274 275 276 277 278 279 280$
     281 282 283 284 285 286 287 288 289 290$
     291 292 293 294 295 296 297 298 299 300$
     301 302 303 304 305 306 307 308 309 310$
     311 312 313 314 315 316 317 318 319 320$
     321 322 323 324 325 326 327 328 329 330$
     331 332 333 334 335 336 337 338 339 340$
     341 342 343 344 345 346 347 348 349 350$
     351 352 353 354 355 356 357 358 359 360$
     361 362 363 364 365 366 367 368 369 370$
     371 372 373 374 375 376 377 378 379 380$
     381 382 383 384 385 386 387 388 389 390$
     391 392 393 394 395 396 397 398 399 400$
     T
SD6  1  1  1  1  1  1  1  1  1  1$
     1  1  1  1  1  1  1  1  1  1$
```

```
     1  1  1  1  1  1  1  1  1  1$
     1  1  1  1  1  1  1  1  1  1$
     1  1  1  1  1  1  1  1  1  1$
     1  1  1  1  1  1  1  1  1  1$
     1  1  1  1  1  1  1  1  1  1$
     1  1  1  1  1  1  1  1  1  1$
     1  1  1  1  1  1  1  1  1  1$
     1  1  1  1  1  1  1  1  1  1$
     1  1  1  1  1  1  1  1  1  1$
     1  1  1  1  1  1  1  1  1  1$
     1  1  1  1  1  1  1  1  1  1$
     1  1  1  1  1  1  1  1  1  1$
     1  1  1  1  1  1  1  1  1  1$
     1  1  1  1  1  1  1  1  1  1$
     1  1  1  1  1  1  1  1  1  1$
     1  1  1  1  1  1  1  1  1  1$
     1  1  1  1  1  1  1  1  1  1$
     1  1  1  1  1  1  1  1  1  1$
     1  1  1  1  1  1  1  1  1  1$
     1  1  1  1  1  1  1  1  1  1$
     1  1  1  1  1  1  1  1  1  1$
     1  1  1  1  1  1  1  1  1  1$
     1  1  1  1  1  1  1  1  1  1$
     1  1  1  1  1  1  1  1  1  1$
     1  1  1  1  1  1  1  1  1  1$
     1  1  1  1  1  1  1  1  1  1$
     1  1  1  1  1  1  1  1  1  1$
     1  1  1  1  1  1  1  1  1  1$
     1  1  1  1  1  1  1  1  1  1$
     1  1  1  1  1  1  1  1  1  1$
     1  1  1  1  1  1  1  1  1  1$
     1  1  1  1  1  1  1  1  1  1$
     1  1  1  1  1  1  1  1  1  1$
     1  1  1  1  1  1  1  1  1  1$
     1  1  1  1  1  1  1  1  1  1$
     1  1  1  1  1  1  1  1  1  1$
     1  1  1  1  1  1  1  1  1  1$
     1  1  1  1  1  1  1  1  1  1$
     1
c
nps 1E06
c
print
```

C.4. Y-90 beta source in the SiC slab geometry using 0.760 MeV as a 1/3 max energy

```
Y-90 beta source in the SiC slab geometry
c Cell card
```

```
1    1  -3.21     -1   imp:e=1
2    0             1   imp:e=0
c Surface card
1 RPP     -100 100 -100 100 0 0.12

c
c Mode card
MODE e
c
c
c
c Materials
m1 estep=300   14000.03e          -0.70045   $ MAT1
               6000.03e           -0.299548  $ SiC
c
c
c Source Definition
sdef PAR=e  DIR=1   POS=0 0 0   VEC=0 0 1   ERG=0.76
c
c Tallies
Mesh Tally
tmesh
 rmesh3 TOTAL
  cora3  -100 100
  corb3  -100 100
  corc3  0 1199i 0.12
endmd
c
nps 1E6
c
print
```

C.5. Y-90 beta source in the SiC sphere geometry using beta energy spectra

```
SiC Sphere with Y-90 beta source at center
c Cell card
1    1  -3.21      -1   imp:e=1
2    0         1   -2   imp:e=0
3    0         2        imp:e=0
c Surface card
1 so 0.3
2 so 1

c Mode card
MODE e
c
c Materials
m1 estep=300    14000.03e          -0.70045   $ MAT1
```

```
               6000.03e          -0.299548  $ SiC
c
c Source Definition
sdef PAR=e  POS=0 0 0  ERG=d1
si1 h 0 227i 2.28
sp1 0 0.003406709 0.003406709 0.003459119 0.00351153  0.003616352
      0.003721174 0.003773585 0.003878407 0.003930818 0.004035639
      0.00408805  0.004140461 0.004245283 0.004297694 0.004350105
      0.004402516 0.004454927 0.004559748 0.004612159 0.00466457
      0.004716981 0.004769392 0.004874214 0.004926625 0.004979036
      0.005031447 0.005083857 0.005136268 0.005188679 0.00524109
      0.005293501 0.005345912 0.005345912 0.005398323 0.005450734
      0.005503145 0.005555556 0.005607966 0.005607966 0.005660377
      0.005660377 0.005712788 0.005765199 0.005765199 0.00581761
      0.00581761  0.005870021 0.005870021 0.005922432 0.005974843
      0.005974843 0.005974843 0.005974843 0.006027254 0.006027254
      0.006027254 0.006079665 0.006079665 0.006132075 0.006132075
      0.006132075 0.006132075 0.006132075 0.006184486 0.006184486
      0.006184486 0.006184486 0.006184486 0.006184486 0.006184486
      0.006236897 0.006236897 0.006236897 0.006236897 0.006236897
      0.006236897 0.006236897 0.006236897 0.006236897 0.006236897
      0.006236897 0.006236897 0.006236897 0.006236897 0.006236897
      0.006236897 0.006236897 0.006236897 0.006184486 0.006184486
      0.006184486 0.006184486 0.006184486 0.006132075 0.006132075
      0.006132075 0.006132075 0.006132075 0.006079665 0.006079665
      0.006079665 0.006079665 0.006027254 0.006027254 0.006027254
      0.006027254 0.005974843 0.005974843 0.005974843 0.005974843
      0.005922432 0.005922432 0.005922432 0.005870021 0.005870021
      0.005870021 0.00581761  0.00581761  0.00581761  0.005765199
      0.005765199 0.005712788 0.005712788 0.005660377 0.005660377
      0.005607966 0.005555556 0.005555556 0.005503145 0.005450734
      0.005450734 0.005398323 0.005398323 0.005345912 0.005293501
      0.00524109  0.005188679 0.005188679 0.005136268 0.005136268
      0.005083857 0.005031447 0.004979036 0.004926625 0.004874214
      0.004821803 0.004821803 0.004769392 0.004716981 0.00466457
      0.004612159 0.004559748 0.004507338 0.004454927 0.004402516
      0.004350105 0.004297694 0.004245283 0.004192872 0.004192872
      0.004140461 0.00408805  0.004035639 0.003930818 0.003878407
      0.003825996 0.003773585 0.003668763 0.003563941 0.00351153
      0.003459119 0.003354298 0.003301887 0.003249476 0.003197065
      0.003197065 0.003092243 0.003039832 0.00293501  0.0028826
      0.002830189 0.002777778 0.002672956 0.002568134 0.002463312
      0.002410901 0.00230608  0.002253669 0.002201258 0.002148847
      0.002044025 0.001991614 0.001886792 0.001834382 0.001781971
      0.00172956  0.001624738 0.001572327 0.001467505 0.001415094
      0.001310273 0.001257862 0.00115304  0.001100629 0.001048218
      0.000995807 0.000943396 0.000890985 0.000838574 0.000786164
      0.000733753 0.000681342 0.000628931 0.00057652  0.000524109
      0.000471698 0.000419287 0.000366876 0.000314465 0.000262055
```

```
      0.000209644 0.000157233 0.000104822 0.000104822 5.24109E-05
      5.24109E-05 5.24109E-05 5.24109E-05
c
c Tallies
Mesh Tally
tmesh
 smesh1:e PEDEP
  cora1  0.0 2999i  0.3
  corb1  180
  corc1  360
endmd
c
nps 1E06
c
print
```

APPENDIX B: CALCULATIONS FOR PREDICTING ENERGY DEPOSITION IN A DEPLETION REGION OF 1 μM THICK FOR THE SLAB AND SPHERE MODELS

PLEASE SEE THE TABLES IN ATTACHED CD

VITA

Kyuhak Oh was born on June 14, 1981, and raised in Nonsan, Chungchongnam-do, Republic of Korea by his parents, Kisoo Oh and Myungja Lee. He has obtained the following degrees: B.S. in applied chemistry and military science (2005) from the Korea Military Academy in Seoul, South Korea, M.S. in Nuclear Engineering (2011) from the University of Missouri in Columbia, USA. Kyuhak will begin work as a captain in the Republic of Korea Army again.